A STUDY ON NEW TURKISH GROUND SNOW LOAD MAP AND SNOW DAMAGE PREVENTION RECOMMENDATIONS FOR SOLAR POWER PLANTS

A THESIS SUBMITTED TO
THE GRADUATE SCHOOL OF NATURAL AND APPLIED SCIENCES
OF
MIDDLE EAST TECHNICAL UNIVERSITY

BY

ÖZLEM TEMEL

IN PARTIAL FULFILLMENT OF THE REQUIREMENTS
FOR
THE DEGREE OF MASTER OF SCIENCE
IN
CIVIL ENGINEERING

JANUARY 2020

Approval of the thesis:

A STUDY ON NEW TURKISH GROUND SNOW LOAD MAP AND SNOW DAMAGE PREVENTION RECOMMENDATIONS FOR SOLAR POWER PLANTS

submitted by **ÖZLEM TEMEL** in partial fulfillment of the requirements for the degree of **Master of Science** i**n Civil Engineering, Middle East Technical University** by,

Prof. Dr. Halil Kalıpçılar
Dean, Graduate School of **Natural and Applied Sciences** _____

Prof. Dr. Ahmet Türer
Head of the Department, **Civil Engineering** _____

Prof. Dr. Ahmet Türer
Supervisor, **Civil Engineering, METU** _____

Examining Committee Members:

Prof. Dr. Cem Topkaya
Civil Engineering, METU _____

Prof. Dr. Ahmet Türer
Civil Engineering, METU _____

Prof. Dr. Eray Baran
Civil Engineering, METU _____

Assoc. Prof. Dr. Tuğrul Yılmaz
Civil Engineering, METU _____

Assist. Prof. Dr. Halit Cenan Mertol
Civil Engineering, Atılım University _____

Date: 31.01.2020

I hereby declare that all information in this document has been obtained and presented in accordance with academic rules and ethical conduct. I also declare that, as required by these rules and conduct, I have fully cited and referenced all material and results that are not original to this work.

Name, Last name : Özlem, Temel

Signature :

ABSTRACT

A STUDY ON NEW TURKISH GROUND SNOW LOAD MAP AND SNOW DAMAGE PREVENTION RECOMMENDATIONS FOR SOLAR POWER PLANTS

Temel, Özlem
Master of Science, Civil Engineering
Supervisor : Prof. Dr. Ahmet Türer

January 2020, 91 pages

Renewable energy sources have become an environment friendly alternative to fossil fuels. As a renewable source, solar energy becomes widespread under favor of decreasing costs in Photovoltaic (PV) cell production. Similar to the growth trend in the world, total production capacity of installed Solar Power Plants (SPP) have recently reached over 5 GW in Turkey. In a typical SPP, PV modules are mounted on steel supporting structures with a site-specific inclination angle. In the last years, damage of many PV mounting structures due to snow load has shown that characteristic ground snow load proposed in design load code TS 498 is not suitable for SPP and does not sufficiently represent regional variance of snow climate. In the present study, snow load values with 50-year mean return interval are obtained using ECMWF- ERA 5 global climate model snow data and a new ground snow load map for Turkey is proposed. Proposed map is validated by meteorological observations and compared with TS 498 snow load values on ground. Some design recommendations are made for PV supporting structures at SPP based on commonly observed snow damage patterns.

Keywords: Solar Power Plant, Snow Load Map, Photovoltaic Panel

ÖZ

YENİ TÜRKİYE ZEMİN KAR YÜKÜ HARİTASI ÜZERİNE BİR ÇALIŞMA VE GÜNEŞ ENERJİSİ SANTRALLERİNDE KAR HASARININ ÖNLENMESİNE İLİŞKİN ÖNERİLER

Temel, Özlem
Yüksek Lisans, İnşaat Mühendisliği
Tez Yöneticisi: Prof. Dr. Ahmet Türer

Ocak 2020, 91 sayfa

Yenilenebilir enerji kaynakları, fosil yakıtlara çevre dostu bir alternatif haline gelmiştir. Yenilebilir bir enerji kaynağı olan güneş enerjisi, düşen fotovoltaik panel maliyetleri sayesinde dünya genelinde yaygın olarak kullanılmaya başlanmıştır. Dünyadaki eğilime paralel olarak, Türkiye'deki güneş enerjisi santrallerinin (GES) üretim kapasitesi 5 GW'a ulaşmıştır. Tipik bir GES'de, PV paneller sahaya özgü bir eğime sahip çelik taşıyıcı yapılara monte edilmektedir. Geçtiğimiz yıllarda panel taşıyıcı yapılarda meydana gelen kar yükü hasarları, tasarım yükü kodu olan TS 498'in GES'ler için uygun olmadığı ve önerilen kar yüklerinin, bölgesel farklılıkları yeterince temsil edemediğini göstermiştir. Bu çalışmada, 50 yıl ortalama tekerrür periyoduna sahip kar yükü değerleri ECMWF'in ERA 5 küresel iklim veri seti kar verileri kullanılarak hesaplanmış ve Türkiye için yeni bir zemin kar yükü haritası önerilmiştir. Önerilen harita, meteorolojik ölçümlerle kıyaslanarak doğrulması yapılmış ve TS 498'de önerilen zemin kar yükü değerleri ile karşılaştırılmıştır. GES'lerde kullanılan PV panel taşıyıcı yapılarda sıklıkla görülen kar hasarlarına ilişkin tavsiyelerde bulunulmuştur.

Anahtar Kelimeler: Güneş Enerjisi Santrali, Kar Yükü Haritası, Fotovoltaik Panel

To my family

ACKNOWLEDGMENTS

First of all, I would like to thank my supervisor Prof. Dr. Ahmet Türer for his guidance, advice, criticism, encouragements and insight throughout the research.

I would like to express my sincere thanks to my husband Ruhi Deniz Yalçın for his cooperation and helps during this thesis and for being my best friend in life.

I would like to express my greatest gratitude to my mother Belgin Toruk for being always on my side, taking care of my little son Tibet Yalçın during my thesis studies with patience, sacrifice and love.

The last but not least, I would like to express my love to my little sunshine Tibet Yalçın. His hugs and smiles always give me courage and cheer.

TABLE OF CONTENTS

ABSTRACT v

ÖZ vi

ACKNOWLEDGMENTS viii

TABLE OF CONTENTS ix

LIST OF TABLES xi

LIST OF FIGURES xii

CHAPTERS

1 INTRODUCTION 1

1.1 Background 1

1.2 Objectives and Scope 7

2 LITERATURE REVIEW 9

2.1 Ground Snow Loads in Turkish Provisions 9

2.2 Determination of Ground Snow Load 10

2.2.1 Measurement of Snow Depth and Snow Water Equivalent 11

2.2.2 Snow Depth-Snow Water Equivalent Conversion 11

2.2.3 Probability Distribution Functions 12

2.2.4 Sources of Uncertainty in Ground Snow Loads 16

2.3 Development of European Snow Load Provisions 17

2.4 Previous Studies on Ground Snow Loads in Turkey 23

2.5 Snow Loads Acting on PV Arrays 24

3 CONSTRUCTION OF PROPOSED GROUND SNOW LOAD MAP 29

3.1 ERA 5 Reanalysis Data 29

3.2 Obtaining Annual Maximum Time Series for Era-5 Data 30
3.3 Obtaining Annual Maximum Time Series for Climate Station Data 31
3.4 Comparison of Annual Maximum Time Series of ERA5 Data and Station Data 34
3.5 Determination of Ground Snow Loads at Grid Points 39
3.6 Determination of Ground Snow Loads at TSMS Stations 47
3.7 Downscaling of Gridded Snow Load Values 47
3.8 Comparison of Ground Snow Loads 49
3.9 Mapping of Ground Snow Loads 49
3.10 Comparison of Proposed Map with TS498 Ground Snow Values 52
3.11 Change Trend in Snow Loads 56
4 RECOMMENDATIONS ON PREVENTION OF SNOW DAMAGE OBSERVED IN SOLAR POWER PLANTS 59
4.1 Typical PV Mounting Structures Used in Turkey 59
4.2 Observed Snow Damage in Solar Power Plants 60
4.3 Recommendations 64
5 CONCLUSIONS AND FUTURE WORK 67
REFERENCES 71
APPENDICES
A. COMPARISON TABLES 75

LIST OF TABLES

TABLES

Table 1- Snow Density Models Used by European Countries adopted from Sanpaolesi (1996) 19
Table 2- Determination of Lognormal Probability Plot..... 40
Table 3- Characteristic Ground Snow Loads kN/m^2 in TS EN 1991-1-3 53

LIST OF FIGURES

FIGURES

Figure 1- Installed Capacity Trend of Solar Energy in Turkey (retrieved from https://www.irena.org/solar).....2
Figure 2- Solar Resource Map of Turkey (retrieved from https://solargis.com/maps-and-gis-data).....3
Figure 3- Damaged PV Mounting Structures, Ekol Loss Adjusting (2018).....5
Figure 4- Usage of snow fences to prevent snow drifting accross a highway (adopted from https://clearroads.org/december-2017/) 6
Figure 5- Snow transport along fetch distance and snow deposition behind snow fence.....7
Figure 6- Ten Climatic Regions in Europe adopted from Sanpaolesi (1996).....21
Figure 7- Example for Zoning-Alpine Region adopted from Sanpaolesi (1996)....22
Figure 8- Shape Coefficient and Drift Length for Flat Roofs with PV Panels suggested by Formichi (2019).....27
Figure 9- Grid points covering Turkey 31
Figure 10- Station Data (Ankara-Esenboğa) Compared to ERA-5 Data (without error correction).....33
Figure 11- Station Data (Ankara-Esenboğa) Compared to ERA-5 Data (with error correction) 33
Figure 12- Correlation between measured SWE at station locations and nearest grid point 35
Figure 13- Correlation between measured SD at station locations and nearest grid point 35
Figure 14- Annual Maximum SWE Time Series of Çorum Station (Station No=17084) and Model Data (R=0.92).....36
Figure 15- Annual Maximum SWE Time Series of Tunceli Station (Station No=17165) and Model Data (R=0.34).....36

Figure 16- Annual Maximum SD Time Series of Sivas Station (Station No=17090) and Model Data (R=0.98) 37
Figure 17- Annual Maximum SD Time Series of Sivas-Kangal Station (Station No=17762) and Model Data (R=0.35)..... 38
Figure 18- Lognormal Tail-Fit vs Lognormal Fit to All Data 42
Figure 19- Ground Snow Values at Grid Points..... 42
Figure 20- Ground Snow Load Contour Map for 50-year MRI..... 44
Figure 21- Ground Snow Load Contour Map for 190-year MRI..... 44
Figure 22- Ground Snow Load Contour Map for 475-year MRI..... 45
Figure 23- Standard Deviation of 50 Year MRI Snow Load Values 46
Figure 24- Coefficient of Variation for 50 Year MRI Snow Load Values..... 46
Figure 25- Best Fitting Altitude Function (a=0.6748, b=1186, R^2=0.46) 48
Figure 26- Mapped Values of Parameter ‘a’..... 50
Figure 27- Mapped Values of Ground Snow Load and Overlapped Figures 51
Figure 28- Ground Snow Load Map of Turkey in TS EN 1991-1-3..... 53
Figure 29- TSMS Stations Used in Comparison Shown on Turkey Map 54
Figure 30- Comparison of Ground Snow Loads of TSMS Stations with Proposed Mapped Values (Model) and Values in Turkish Provisions (TS498) 54
Figure 31- Percent Difference between TS498 Values and Proposed Values for City Centers..... 56
Figure 32- Change Trend in Annual Maximum Snow Load Over the Course of 40 years (1979-2018)..... 57
Figure 33- Typical View of PV Mounting Structures 59
Figure 34- Snow Accumulation on PV Panels-1..... 61
Figure 35- Snow Accumulation on PV Panels-2..... 61
Figure 36- Snow Accumulation on PV Panels-3..... 61
Figure 37- Damaged Main Beam-1 62
Figure 38- Damaged Main Beam-2 63
Figure 39- Buckling of Main Beam under Dead Load+Snow Load 63

CHAPTER 1

INTRODUCTION

1.1 Background

In recent years, renewable and environment-friendly sources of energy have been used widely in the world due to increased environmental concerns related with global warming. Moreover, developing countries with increasing energy demand and limited energy sources (natural gas, petroleum etc.) are in search of alternatives to fossil fuel based energy sources to lower energy related costs.

Main renewable energy sources are wind energy, hydropower, geothermal energy, solar energy, and biomass energy. Among different kind of renewable energy sources, solar energy investments boosted around the world thanks to decrease in PV panel prices. According to International Renewable Energy Agency (IRENA) (2019), price of Photovoltaic (PV) panels decreased by 80% since 2009 while wind turbine prices decreased almost 30-40%.

As stated by Ministry of Foreign Affairs (2019), Turkey's energy demand has been increasing with an annual growth rate of 5.5% since 2002, which is the fastest growth rate among OECD member countries and energy consumed in Turkey is highly dependent on import energy sources. Thus, a new energy strategy has been developed by Turkey in order to reduce dependency on import energy sources based on fossil fuels and increase contribution of renewable energy in total electricity production. In this perspective, Turkey became a founding member of IRENA in 2009 and a renewable energy support mechanism was established in 2011 in order to encourage investments on renewable energy sector. Following this advances, solar energy systems have become the most widely accepted renewable energy type in

Turkey (Uyan, 2017). Figure 1 shows rapid growth of installed solar power capacity in Turkey in recent years.

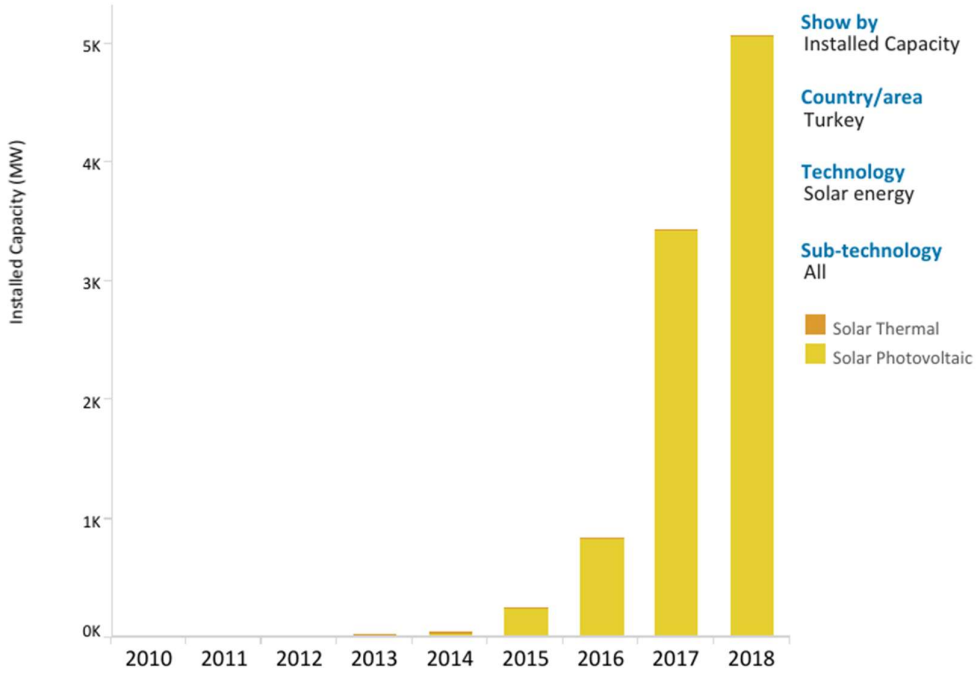

Figure 1- Installed Capacity Trend of Solar Energy in Turkey (retrieved from https://www.irena.org/solar)

In a photovoltaic solar power plant, PV panels convert solar energy into electricity. PV arrays, composed of interconnected PV panels, are mounted on a structure which keep them in correct position to optimize electricity production and provide a structural support. Typically fixed angle arrays are used since they require lower initial and maintenance costs than arrays in which one or two axis sun tracking system is used. Mounting structure constitutes almost 10% of initial investment however more importantly it carries PV panels, which constitute about 50-60% of investment.

Electricity produced by PV panels depends on amount of solar irradiance. According to solar resource map in Figure 2, southern regions have a higher solar energy

production potential compared to Marmara and Black Sea regions. Therefore, most of solar power plants in Turkey are located in southern regions. In addition to amount of solar irradiance of candidate site, there are many parameters considered by investors in feasibility stage such as availability of site regarding agricultural activities and land prices. Some investors prefer foothills of mountains and sloped areas where agricultural activity is limited and land prices are favorable compared to areas located in plains. This preference leads to snow related problems in solar power plants due to high correlation between snow load and altitude.

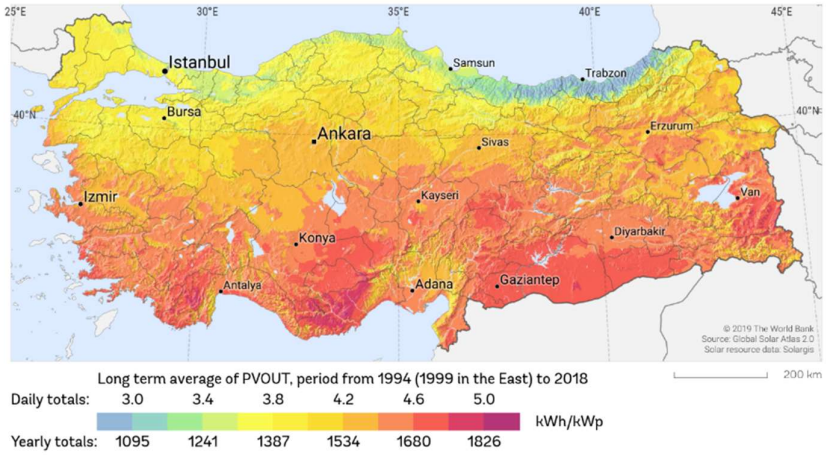

Figure 2- Solar Resource Map of Turkey (retrieved from https://solargis.com/maps-and-gis-data)

Following 2015, when solar power plant constructions had just to become widespread (Figure 1), snow damage has begun to been observed in many recently built solar power plants in Turkey. According to report prepared by insurance company, Ekol Loss Adjusting (2018), in 2016-2017 winter season, many steel PV mounting structures, especially in Konya, Kayseri, Kahramanmaraş cities of Turkey, heavily damaged or collapsed due to weight of accumulated snow (Figure 3). Some of the reported reasons of damage related with snow were summarized as follows:

- Ground snow load observed at the site were greater than snow load value given in TS498.
- Snow load regions defined in TS498 were not correctly selected in snow load calculations and statement about increase in snow load for altitudes above 1000 m was disregarded.
- TS 498 covers loads on building like structures and is not suitable for Solar Power Plants (SPP) supporting structures.
- Damaged plants were sited in foothills of mountainous regions where snow transportation from hills by wind and accumulation on ground between and over SPP were observed. However, simple structures in the same area with flat roofs had drastically lower amount of snow thickness accumulated on their roofs.
- Geometric shape of PV arrays acted as snow trapping blockage and led to heavy snow accumulation between PV arrays.

Figure 3- Damaged PV Mounting Structures, Ekol Loss Adjusting (2018)

Steel PV mounting structures in solar power plants are lightweight steel structures with lower dead load compared to conventional building type structures. Lightweight structures with high snow load to dead load ratio are vulnerable to snow related failures (Holicky & Sykora, 2009). Thus, determination of snow loads accurately becomes more important for lightweight structures and leads to questioning ground snow load values provided by design standards.

In addition to accurate determination of ground snow load, determination of amount of snow transported by wind is very important to approximate snow load acting on structures in reality. Structures or structural parts standing on the way of wind create

aerodynamic shade regions for windblown snow and snow drift occurs. Amount of drifting snow depends on snow flux which is limited by amount of driftable snow and wind (O'Rourke & Wikoff , 2014). Snowdrift between PV panel arrays is very similar phenomenon to snow accumulation created by a snow fence. Snow fences are long and fixed standing structures generally made from aluminum or steel and placed perpendicular to prevailing wind direction to control snow drift and prevent drifting across a highway (ADOT, 2014) (Figure 4). Snow fences reduce wind speed and wind force on the snow surface leading snow particles originally located in a fetch distance and then carried by wind to slow down and come to rest. While some of the particles accumulated on the windward side of the fence, most of snow particles deposit on downwind side of the fence (Tabler & Associates, 1991) (Figure 5).

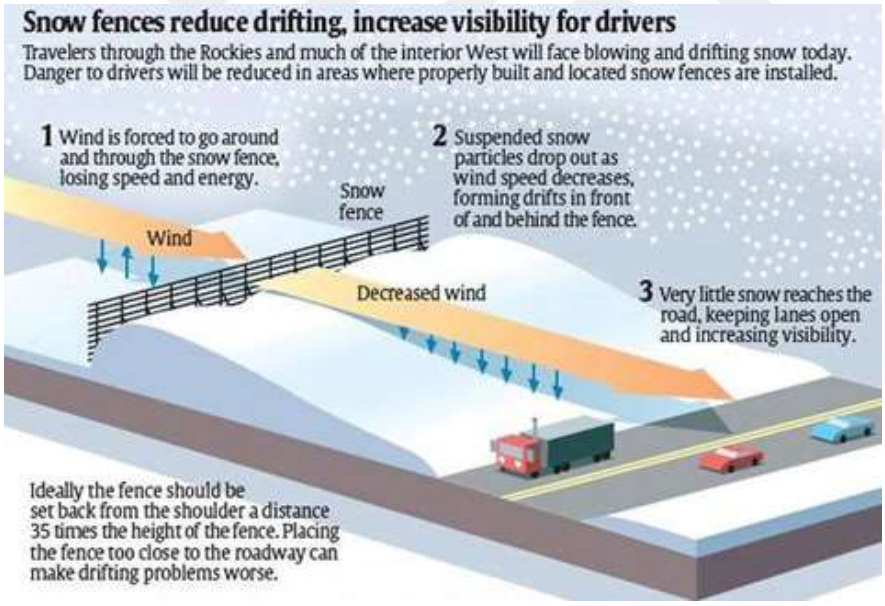

Figure 4- Usage of snow fences to prevent snow drifting accross a highway (adopted from https://clearroads.org/december-2017/)

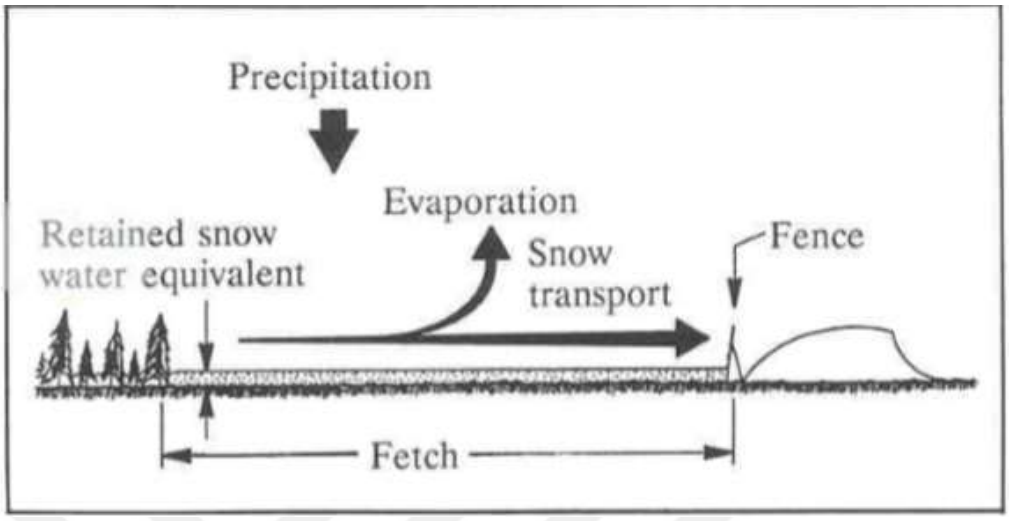

Figure 5- Snow transport along fetch distance and snow deposition behind snow fence (adopted from (Tabler & Associates, 1991))

In the light of aforementioned information, it is clear that number of solar power plants in Turkey will increase due to both increasing energy need and high solar energy potential available. Financial losses related with damage or collapse of solar power plants due to snow loads will increase unless a more realistic snow load is considered in structural design.

1.2 Objectives and Scope

The primary aim of this study to improve accuracy of snow load calculations for solar power plants. For this purpose, ground snow load values provided by TS498 are questioned and a new map is proposed using snow data between 1979-2018 taken from ERA5 climate reanalysis provided by European Centre for Medium-Range Weather Forecasts (ECMWF). Proposed map is then validated by comparing mapped values with snow loads calculated using observation of meteorological stations belong to Turkish State Meteorological Service (TSMS). In addition, a comparison with current snow map in TS498 and national annex of TS EN 1991-1-3 is performed.

Secondly, recommendations are given to prevent snow damage in solar power plants regarding calculation of snow loads acting on PV mounting structures. Since there is no specific standard or guideline on calculation of snow loads acting on PV mounting structures of solar power plants in literature, recommendations made are constituted by making inference from standards or guidelines belong to similar structures.

CHAPTER 2

LITERATURE REVIEW

2.1 Ground Snow Loads in Turkish Provisions

Characteristic value of snow on the ground at the relevant site, s_k is defined as "snow load on the ground based on an annual probability of exceedance of 0.02, excluding exceptional snow loads" in TS EN 1991-1-3.

In Turkey, TS 498 (Design Loads for Buildings) is an active standard for design loads which was prepared based on BSI Code of Basic Data for the Design of Building, DIN 1055 and DIN 18196. However, TS 498 may need recent revisions since it was accepted as a standard in 1987 and revised in 1997 by Turkish Standardization Institute (TSE). In 2007, EN 1991-1-3 (Eurocode 1 - Actions on structures - Part 1-3: General actions -Snow loads) was translated in Turkish and adopted as a valid standard by TSE and named as TS EN 1991-1-3.

EN 1991-1-3 gives guidance to determine the values of loads due to snow to be used for the structural design of buildings and civil engineering works. Some parameters which are called as Nationally Determined Parameters are left open to national choice and reference is given to National Annex. In National Annex of TS EN 1991-1-3, snow map of Turkey and table providing characteristic ground snow load values s_k taken directly from TS 498 are provided.

According to valid regulation in Turkey, "Principles on Design, Calculation, and Construction of Steel Structures" (Çelik Yapıların Tasarım, Hesap ve Yapımına Dair Esaslar) (2018); in structural design of steel structures, characteristic load values

should be determined in accordance with TS498 and snow loads provisions in TS EN 1991-1-3 should be taken into consideration.

2.2 Determination of Ground Snow Load

Ground snow load is defined as the weight of snow on the ground surface in IBC (2012). In general, ground snow load values are determined using data collected by meteorological stations. Snow water equivalent and snow depth measurements are primary data needed when calculating snow load values. Snow water equivalent measurements can be used directly to calculate snow load value however snow depth measurements have to be converted into snow load after taking into account snow density. Snow density depends on many climatic factors and varies among different geographical regions thus there is no single mathematical expression used for snow density calculation in literature. Unfortunately, many meteorological stations in Turkey, as in the world, measure only snow depth data.

Length of annual maximum records is very important for reliability of statistical analysis. According to German investigation based on 94-years snow depth record, ground snow load design values derived from measurements of 30 consecutive winters were yet influenced by exceptional years in the data. Thus it is suggested to use a record length of 40 to 50 years to determine ground snow load values with 50-year Mean Recurrence Interval (MRI) (Sanpaolesi, 1996).

In this study, snow parameters provided by ERA5 climate reanalysis is used instead of records of meteorological stations since it provides data from 1979 to present. Detailed description of ERA5 data and methodologies of conventional snow depth and snow water equivalent measurement are provided in the following sections.

2.2.1 Measurement of Snow Depth and Snow Water Equivalent

In Turkey, Turkish State Meteorological Service (TSMS) and General Directorate of State Hydraulic Works (DSI) collect snow data. Physical properties of snow such as snow depth, snow water equivalent and snow density are observed and archived. In this study, data belong to TSMS archives is used for comparison purposes.

Snow depth is defined as total depth of snow (including any ice) on the ground at the normal observation time. The snow depth includes new snow that has fallen combined with snow already on the ground. It is measured once per day at scheduled time of observation with a measuring stick if there is snow on the ground. Several readings are made and average of these measurement is recorded as snow depth value at measurement location (Snow Measurement Guidelines for National Weather Service Surface Observing Programs, 2013).

Snow water equivalent is defined as the water content of new and old snow on the ground measured by taking a core sample. Core sample is taken from the total snow on the ground which is new snow that has fallen within 24 hours in addition to old snow already on the ground. After sampling, sample snow is melted and amount of water obtained is measured (Snow Measurement Guidelines for National Weather Service Surface Observing Programs, 2013).

As stated in previous section, most climatic stations in Turkey measure snow depth; on the contrary there are few stations measuring snow water equivalent. Thus, a conversion from snow depth to snow water equivalent is needed in order to calculate snow load.

2.2.2 Snow Depth-Snow Water Equivalent Conversion

Various models have been used for conversion of snow depth to snow water equivalent. Since snow load can be directly calculated using snow water equivalent, it is important to determine snow water equivalent accurately.

$$SWE = d\frac{\rho_s}{\rho_w} \quad (1)$$

where SWE is snow water equivalent in m, d is snow depth in m, ρ_s is snow density in kg/m^3, and ρ_w is density of water in kg/m^3 which is approximately (1000 kg/m^3).

Snow density is a complex parameter. It is generally assumed with rule of thumb 10:1 (an assumed snow density of 100 kg/m^3); however, snow density depends on in-cloud (crystal form and size), sub-cloud (sublimation and melting processes), and surface processes (structure of snowpack and degree of compaction regarding wind etc.) and it can vary from 3:1 to 100:1 (Roebber, Bruening, Schultz, & Cortinas Jr., 2003).

2.2.3 Probability Distribution Functions

Since occurrence of snowfalls, the duration and intensity of snow loads have a random nature; investigations of snow should be undertaken on a stochastic basis (Sanpaolesi, 1996). According to the design philosophy of Eurocodes, the European Snow Map represents only extreme values of snow load, namely values with return period of 50 years (Sanpaolesi, 1996).

Selection of Probability Distribution Function (PDF) used for modeling distribution of annual maximum time series of snow load data depends mainly on climate and geographical conditions at meteorological station location. (Ellingwood & Redfield, 1983). Thus, there are various types of PDFs proposed to be suitable for modeling annual maximum ground snow load for different regions.

Ellingwood & Redfield (1983) suggest that the Lognormal distribution fits the observed values of the annual maximum snow load better than any other extreme value distribution for most of evaluated weather stations in US and ASCE/SEI 7-10 was developed based on lognormal distribution.

In scientific research program carried out in order to obtain European Ground Snow Load Map; Extreme value distribution Type I for maximum (Gumbel), Extreme

value distribution Type II for maximum, Weibull (extreme value distribution Type III for minima), Lognormal distribution, and Normal distribution were considered as candidates for best fitting distributions (Sanpaolesi, 1996).

DeBock, Liel, Harris, Ellingwood, & Torrents (2017) developed a new approach to determine design ground snow loads based on uniform risk or reliability instead of uniform hazard (constant return period) approach in which design loads have 2% annual probability of exceedance for all locations and which is used in many standards including ASCE Standard 7-10. In that study, it was stated that despite high importance of tail portion for return periods of 100-1000, it is also very important even with 50-year return periods since tail portion of data directly affects design value. It was also noted that, for especially short historical records, best fitting probability distribution for extremes of the data can be different than the distribution which gives best fit in overall. Thus a 'tail-fitting' approach was applied by fitting a Lognormal distribution to top 33% portion of the data ensuring that at least 10 data points are used considering 30 years of record which was the minimum record length used in their study. Ground snow loads predicted by Lognormal tail fitting was compared with Lognormal distribution fitted to overall data. It was obtained that Lognormal distribution fitted to all data set diverges from largest recordings and underpredicts the ground snow load. Moreover; tail-fitted Normal, Lognormal, Gamma, Log-gamma probability models are compared with Extreme Value Type-II which was the best fitting distribution among distributions fitted to entire data set. Results showed that there were only a 6% range in predictions of 50-year ground snow load values obtained using five different models.

Since 2-parameter Lognormal distribution is used in this study, detailed explanation of Normal Distribution, which is basis for Lognormal Distribution, and Lognormal Distribution are provided in the following section. Reasons for this choice is explained in Chapter 3. In addition, probability plot concept is also explained since it is a commonly used visualization technique to assess goodness of fit of a candidate distribution and also enables determining location and scale parameters of distribution.

2.2.3.1 Normal Distribution

A continuous random variable X is said to have a normal distribution if the probability distribution function of X can be expressed as:

$$f(x;\mu,\sigma) = \frac{1}{\sqrt{2\pi}\sigma} e^{\frac{-(x-\mu)^2}{2\sigma^2}} \qquad -\infty < x < \infty \qquad (2)$$

$$F(x;\mu,\sigma) = \int_{-\infty}^{x} \frac{1}{\sqrt{2\pi}\sigma} e^{\frac{-(x-\mu)^2}{2\sigma^2}} dx \qquad (3)$$

with shape parameter μ and location parameters σ, which are mean and standard deviation of X.

2.2.3.2 Standard Normal Distribution

A normal distribution with μ=0 and σ=1 is called the standard normal distribution. A random variable having a standard normal distribution is called a standard normal variable and is denoted by Z. Probability distribution function of Z is expressed as:

$$f(z;0,1) = \frac{1}{\sqrt{2\pi}} e^{\frac{-z^2}{2}} \qquad -\infty < x < \infty \qquad (4)$$

Cumulative distribution function of Z is;

$$F(z;0,1) = \int_{-\infty}^{z} \frac{1}{\sqrt{2\pi}} e^{\frac{-z^2}{2}} dy \qquad (5)$$

Cumulative distribution function of nonstandard normal distribution can be expressed by using a standardized variable. If X has a normal distribution with mean μ and standard deviation σ, then standardization is obtained by:

$$Z = \frac{X-\mu}{\sigma} \qquad (6)$$

Thus cumulative probability distribution of a nonstandard variable X can be calculated as:

$$F(x;\mu,\sigma\ ) = \Phi\left(\frac{X-\mu}{\sigma}\right) \quad (7)$$

2.2.3.3 Lognormal Distribution

A nonnegative random variable X is said to have a lognormal distribution if the random variable has a normal distribution. Probability distribution function and cumulative probability distribution function of lognormal distribution is expressed as:

$$f(x;\mu,\sigma) = \frac{1}{\sqrt{2\pi}\sigma x} e^{\frac{-[\ln(x)-\mu]^2}{2\sigma^2}} \quad (8)$$

$$F(x;\mu,\sigma) = \Phi\left(\frac{\ln(x)-\mu}{\sigma}\right) \quad (9)$$

where shape and location parameters μ and σ are mean and standard deviation of ln(X).

2.2.3.4 Lognormal Probability Plot

A probability plot is graphical tool used to assess goodness of fit of a candidate distribution and also to determine its parameters. Special axes which are scaled for selected distribution are used in probability plots and rank ordered observations are plotted against their cumulative frequency (Montgomery & Runger, 2018). Construction of Lognormal probability plot is summarized by Burstmaster & Hull (1997) as follows:

- observations are sorted from smallest to largest as $x_1, x_2,\ldots, x_n$ where x_1 is the minimum and x_n is the maximum of data.
- sorted observations are transformed by taking logarithm such as $\ln x_1, \ln x_2,\ldots, \ln x_n$.
- n empirical cumulative probability, $p_1, p_2,\ldots, p_n$, are determined using plotting position formula which has a general form given in equation (12)

and where i is order of data point and a value changes depending on chosen distribution. For Lognormal distribution; Blom (a=0.375), Gringorten (a=0.44), and Weibull (a=0) plotting positions are recommended (Mehdi & Mehdi, 2011).

$$\frac{i-a}{n+1-2a} \tag{10}$$

- z (p_i), inverse cumulative distribution function $\Phi^{-1}(p_i)$, is calculated for each data point.
- $\ln x_1, \ln x_2, \ldots, \ln x_n$ values are plotted against $\Phi^{-1}(p_1)$, $\Phi^{-1}(p_2), \ldots, \Phi^{-1}(p_n)$.
- parameters of Lognormal distribution can be interpreted by fitting a least squares regression line to obtained plot. Reciprocal of the slope of the fitted line gives estimated standard deviation and location of x-intercept gives mean value of Lognormal distribution.

2.2.4 Sources of Uncertainty in Ground Snow Loads

There are two main sources of uncertainty in determined ground snow loads. First one is measurement uncertainty and the other is statistical uncertainty related with selected probability distribution function and determination of its parameters (Rózsás & Sýkora, 2016). Probabilistic models are typically fitted to measurement data without considering their uncertainty however; uncertainty range can reach 50% of the measured snow depth (Rózsás & Sýkora, 2016). Even in automated systems, measurement errors for solid precipitation can range from 20% to 50% due to undercatch in windy weather (Rasmussen, et al., 2012). World Meteorological Organization suggests that solid precipitation should be adjusted for wetting loss, evaporation loss, and wind induced undercatch and wind speed is found to be the most important environmental contributing factor to the systematic undermeasurement of solid precipitation (Goodison, Louie, & Yang, 1998).

Statistical uncertainty arises from the selection of distribution function and the identification of unknown parameters of distribution function (Rózsás & Sýkora, 2015). Rózsás & Sýkora (2015) investigated statistical uncertainty using snow data from Carpathian region. In this study, 2- parameter Lognormal, 3-parameter Lognormal, Gumbel, Generalized Extreme Value distributions; and generalized method of moments, maximum likelihood, and Bayesian parameter selection approaches are used to calculate point estimates with 50, 100, 300, and 1000 year return periods. It was found that uncertainty increases with increasing return period however even for 50-year return period which has lowest uncertainty, point estimate calculated using Gumbel distribution with maximum likelihood parameter estimation method is 1.4 larger than point estimate calculated using 2-parameter Lognormal distribution with Bayesian parameter estimation. Thus it was concluded that uncertainty in probabilistic calculations can lead to underestimation of loads which is extremely important especially if limited number of observations is available.

2.3 Development of European Snow Load Provisions

European Snow Loads Research Program was carried out in 1996-1999 under the contracts to the European Commission DG III-D3. The main scope of the program was improving scientific knowledge on snow loads and determination of snow loads on buildings by producing a sound common scientific basis which could be accepted by all European countries involved in the drafting of Eurocodes.

In that work, practice in eighteen European countries at that time such as type of data recorded, statistical methods being used were reviewed and a new methodology suitable for all countries was developed. Tremendous effort was made to unify different approaches of countries and there were many problems encountered such as different historic record lengths and periods, need for checking huge data for errors, gathering data from different intuitions in same country.

In the Final Report-I, Sanpaolesi (1996), prepared as a product of studies of research program, it is stated that most countries measure snow depth however only a few countries (Germany, Finland, Switzerland, partially UK) measure snow water equivalent. Moreover, in countries where snow water equivalent is measured, number of stations measuring snow water equivalent and their geographical locations provided insufficient data in order to determine snow load values throughout the countries of interest. Thus, snow depth measurements were converted to snow water equivalent using snow density. It was observed that each European country use its own snow density formula for conversion such as a fixed value for the mean density of snow, density as a function of snow depth, density as a function of the place of observation, density as a function of time. In the subject research program, for some countries density model already being used was used and for some new models were elaborated. Snow density models used in research program are shown in Table 1.

Table 1- Snow Density Models Used by European Countries adopted from Sanpaolesi (1996)

No.	CEN member	Density (kg/m^3)
1	Austria	250-300 altitude less than 1500 m above the sea level 350 altitude greater than 1500 m above sea level
2	Belgium	150
3	Denmark	Canadian snow pack model of Leaf/Brink, 200 - for naturally packed snow
4	Finland	Direct measurements of water equivalent, ≈ 250
5	France	150
6	Germany	Snow load factor of German Meteorological Office (DWD) $D = 159.81 + 129.82\,h - 81.09\,h^2 + 59.907\,h^3 - 20.652\,h^4$ for $h < 1.53$ m $D = 270$ for $h \geq 1.53$ m
7	Greece	125
8	Ireland	156.82
9	Iceland	The research group has converted depths to snow loads on the basis of a relation between snow depths and densities varying between 400 and 500 kg/m^3 indicated in a report from the Icelandic Meteorological Institute.
10	Italy	For low altitude: 250 For high altitude time-dependent model is used: 215 - 315 initial density value 315 mean density value in the constant period of the winter 315 - 515 increasing density value at the melting period
11	Luxembourg	150
12	Netherlands	100
13	Norway	225 - 325 for maximum depth occurring in December to May
14	Portugal	no data Spanish data assumed
15	Spain	During the period of maximum snow load: 100 ÷ 500 - for altitude from 1500 to 2000 m 100 ÷ 270 - for altitude from 1000 m to 1500 m 100 ÷ 200 - for altitude from 800 m to 1000 m
16	Sweden	Different values for different parts of country: 230 - for Norrland to Dalsland (Internal, partly mountainous) 280 - for Götaland's coast, Gotland and Öland (islands) 240 - for remaining parts of Sweden
17	Switzerland	100 - for the new-fallen snow 200 - for snow after several hours or days since snowfall 300 - average value at maximum snow load 350 - old snow (after weeks or months since snowfall) 400 - wet snow
18	UK	156.82

Characteristic snow load was defined as snow load which as a probably of exceedance of 0.02 within any one year and this corresponds to a MRI of 50 years. After obtaining record of ground snow loads using snow density models proposed for each country, next step was determining characteristic snow loads at station locations. It was considered that annual maximum of each year of observation belongs to an underlying extreme value distribution and using best fitting distribution, characteristic snow load value can be calculated. However, length of records was generally insufficient to confidently estimate 50 year MRI snow loads by using extreme value statistics. Thus, in most of the cases, records covering a

minimum total number of winters of 40-50 years were used and it was stated that records less than 20 years are not sufficient to estimate 50 year MRI snow loads.

It is said that characteristic value of snow load is very sensitive to choice of probability distribution fitted to annual maximum snow load data and best fitting probability distribution function primarily depends on climatic and geographical conditions at the meteorological station. After investigation of performance of different probability distribution functions, it was decided to use Gumbel (extreme value distribution Type-I) for whole Europe despite the fact that in some regions such as Germany and Switzerland best fitting distribution deviates from Gumbel.

In some countries especially ones located in coastal and southern Europe, "individual event" and "mixed distribution" approaches were proposed to take into account probability of no-snow years. There were also some countries which has exceptional snow loads, belong to infrequent snowfalls leading significantly greater snow load, that did not fit well with the remainder of the data set. For this case, if ratio of largest load value to the characteristic load determined without the inclusion of that value is greater than 1.5 then the largest load was defined as an 'exceptional load'.

After obtaining characteristic snow load values at each station location, a snow load map was constituted. Instead of setting up a map which gives characteristic values directly, defining areas in which a given altitude function would be applied was preferred since such a map would have to be very detailed in mountainous parts of Europe and would follow topographical pattern.

In the mapping process, firstly, major climatic regions in Europe were identified taking into account a combination of reasons and factors such as physical boundaries. It was assumed that the snow loads observed within the same climatic region are due to similar meteorological conditions. Ten climatic regions determined are shown in Figure 6. Secondly for each region, best fitting altitude function was found using all data points in the subject region. Although in some regions, there were no clear correlation between snow load and altitude such as Iceland and Norway, in most of

climatic regions there were good correlation. Comparing correlation coefficients obtained for different functions in each region, one parabolic (11) and one linear (12) function are selected. However, it is stated that selected parabolic or linear function represents average increase of snow load with altitude. Thus, varying the first parameter 'a' and keeping parameter 'b' constant in a region, best fitting function was replaced by several curves which represent relationship for different zones defined in each region as shown in Figure 7. Average function of upper and bound functions was determined as zone function acknowledging approximately half of the stations would have a snow load larger than value given by the function.

$$s_k = a\left[1 + \left(\frac{A}{b}\right)^2\right] \tag{11}$$

$$s_k = a + \frac{A}{b} \tag{12}$$

where A is altitude above sea level (m), a (kN/m^2) and b (m) are parameters of the function and s_k (kN/m^2) is characteristic snow load.

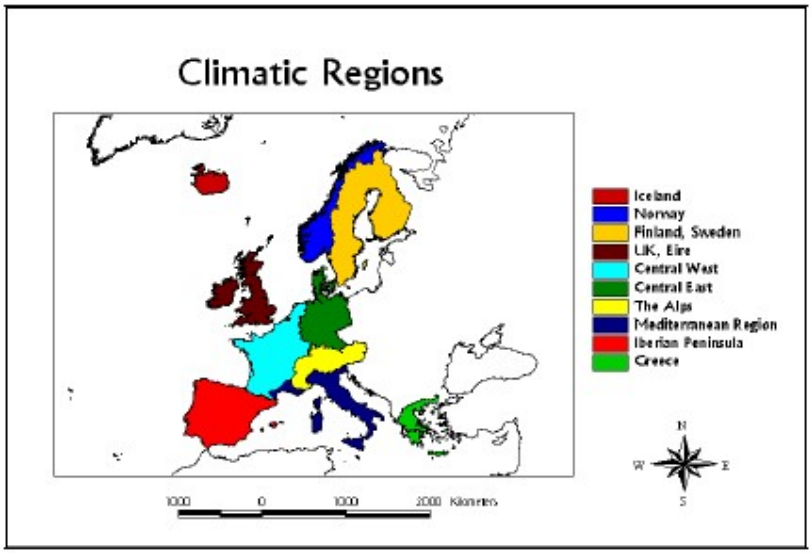

Figure 6- Ten Climatic Regions in Europe adopted from Sanpaolesi (1996)

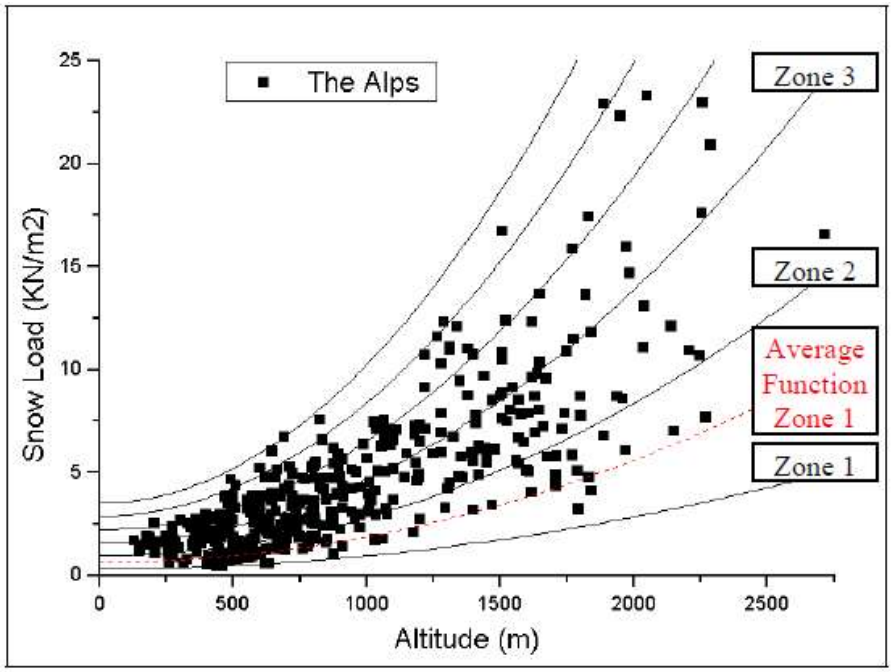

Figure 7- Example for Zoning-Alpine Region adopted from Sanpaolesi (1996)

In order to obtain zone maps, a values were interpolated by inverse distance weighting to a regular grid. Then, $(a_{max} - a_{min})/NZ$ was used for contouring where a_{max} and a_{min} are maximum and minimum 'a' parameters in the region and NZ is number of zones. As a result, for a specific zone Z where altitude-snow load relationship shows parabolic relationship, snow load was represented as follows:

$$s = \left(a_{min} + [Z - 0.5] * \frac{[a_{max} - a_{min}]}{NZ}\right)[1 + \left(\frac{A}{b}\right)^2] \qquad (13)$$

At the present time, due to increased number roof failures in Europe, there are studies on snow load provisions of Eurocode regarding effect of global warming. According to technical report "Towards new European Snow Load Map" (Croce, et al., Towards New European Snow Load Map, 2016), second generation of Eurocodes is expected by 2020 and although no new maps taking into consideration effects of climate

change is planned, actions related with climate change is planned be involved in design rules. In the Final Report of Project Team on SC1.T5 “Climate change” (2017), it was concluded that science of climate change needs improvement to be used in quantification of extreme values thus it was recommended that weather parameters important for determination of characteristic values should be re-examined at regular intervals not exceeding 10 years.

2.4 Previous Studies on Ground Snow Loads in Turkey

Özgen (2007) constituted a ground snow load map by using snow data belong to Turkish State Meteorological Service (TSMS). In this study, meteorological stations are divided into two and stations measuring snow water equivalent and snow depth together are named as first order stations whereas stations measuring only snow depth are named as second order stations. Data belong to 64 first order stations and 36 second order stations with minimum 30 years of data except 17 second order stations with minimum 15 years of data were used in statistical analysis. When data obtained from stations were deeply investigated, it was observed that there were many missing data in many stations. In order to obtain a complete dataset, correlation between stations were determined and station showing best correlation with station having incomplete data was used to complete missing data. After obtaining complete dataset of each station, Lognormal, Gumbel, and Weibull probability distribution functions were fitted to annual maximum data series of each station. Best fitting distribution was selected using probability plot correlation coefficient test in order to determine 50 year MRI ground snow load values at station locations. For second order stations, since snow load values could not be determined using snow depth values directly, relationship between 50 year MRI ground snow load values and 50 year MRI snow depth values obtained by a regression analysis in first order stations were used. After obtaining ground snow load values at station locations, data normalization technique was applied and normalized values are regionalized using inverse distance weighting spatial interpolation method. Obtained ground snow load

map was compared with ground snow load values given by TS498 and it was concluded that for 52% of city center in Turkey TS 498 values were higher than values in proposed map, for 14% values were similar and for 34% TS498 values were much lower than values in proposed map.

Durmaz & Daloğlu (2014) evaluated design ground snow load values in Turkish Standards by comparing their results obtained by statistical analysis of snow data belong to 92 climatic stations of TSMS measuring snow depth (second order stations) and 60 stations measuring snow water equivalents (first order stations). Using minimum 30 years of data best fitting probability distribution was selected among Gumbel, Lognormal, and Weibull distributions by using probability plot correlation coefficient test. 50-year MRI ground snow loads were calculated from first order stations and 50-year MRI snow depth values were calculated for second order stations. Results were compared with TS 498 values and it was concluded that TS 498 recommends uneconomical ground snow load values for 71.7% of city centers with almost no snowfall or city centers with no severe snowfall occurrences. For 28.3% of city centers which are mainly located in regions with severe winter conditions, TS 498 ground snow loads were found to be unsafe. It was also concluded that for some places ratio between calculated ground snow load and TS 498 value was larger than 2.24 which is larger than safety factor for steel structures, 1.67, in TS 648 (Turkish Standard used in design of steel structures).

2.5 Snow Loads Acting on PV Arrays

In general, PV panels are mounted on rooftops, ground or facades of structures to produce electricity. In solar power plants, ground-mounted systems are used and PV panel arrays are mounted on frames attached to ground.

In many building codes, roof snow loads are estimated by multiplying ground snow load s_k with certain coefficients considering geometry, exposure, and thermal properties of the roof. Although there are few provisions related to snow loads acting

on roofs with PV panels on top, there is no specification providing guidance for ground mounted PV arrays. Recommendations and specifications related with snow loads acting on PV panels are focused on design of roof and snow accumulation on different parts of the roof due to installation of PV panels. For example, International Building Code (IBC) and International Residential Code (IRC) have specific sections for design and construction of roofs with PV panels and IBC (2015) states in section *1607.12.5.2-Photovoltaic Panels or Modules* that "where applicable, snow drift loads created by photovoltaic panels or modules shall be included".

O'Rourke & Isyumov (2016) published recommendations on snow load provisions of ASCE 7-10 named as "Snow Loads on Solar-Paneled Roofs" which was based on limited case stories, laboratory studies, design criteria, and engineering judgement. In that document, balanced, sliding, and drift snow load cases defined in ASCE 7-10 were described for roofs with solar panels on top. However, snow load on PV array itself was not the subject of the document thus recommendation provided were focused on effect of existence of solar panels to snow loads acting on the roof.

EN 1991-1-3 provides guidance for structural design of buildings and snow loads acting on roofs with PV arrays are not covered in current version. Thus, snow loads acting on mounting structures are performed considering the structure itself as an inclined roof in practice. Among roof types provided in EN 1991-1-3, mounting structure of PV panels can be considered as a multi-span roof.

In EN 1991-1-3 two load arrangements are defined as undrifted and drifted snow on roofs and two design situations are defined as persistent/transient and accidental design situations. There are also exceptional conditions defined as exceptional falls and exceptional drift. Design situations and load arrangements to be used in different locations are tabulated in Annex A of EN 1991-1-3. Undrifted roof snow load is uniformly distributed on the roof and only affected by the shape of the roof. Whereas, drifted snow load is a result of distribution of snow due to change in location of snow on the roof caused by other actions such as wind. For roofs in which sliding snow is

prevented such as roofs with parapets, minimum snow load shape coefficient, μ_i, is limited to 0.8.

For a normal case with no exceptional falls or drift, under persistent/transient design situation undrifted and drifted roof snow loads are defined in EN 1991-1-3 as follows:

$$s = \mu_i C_e C_t s_k \quad (1)$$

where;

s is roof snow load

μ_i is the snow load shape coefficient (differs for drifted and undrifted load arrangements)

C_e is the exposure coefficient

C_t is the thermal coefficient

s_k is the characteristic value of snow load on the ground

During the ongoing review studies of Eurocode, a model was proposed by Formichi (2019) about snow load distribution on flat roofs with PV arrays to be used in new version of EN 1991-1-3. In this model, for PV arrays having a row spacing less than two times the height of solar panels, an increased shape coefficient, μ_x, is suggested in order to represent snow drift caused by solar panels. The model suggested by Formichi is summarized by Grammou, Pertermann, & Puthli, 2019 (2019) as follows:

$$\mu_x = 1 \leq \gamma \frac{h}{s_k} \leq 4$$

where;

μ_x increased shape coefficient for length l_1 according to Figure 8

l_1 Panel-covered roof length including gaps according to Figure 8

l_s Drift length at the borders to length l_1 with $l_s = 2h/C_e$

b distance or gap between two rows of panels in meters

h height of solar panels in meters

C_e exposure coefficient, with $0.8 \leq C_e \leq 1.2$

γ equivalent density by weight in kN/m^3

s_k characteristic snow load on the ground in kN/m^2

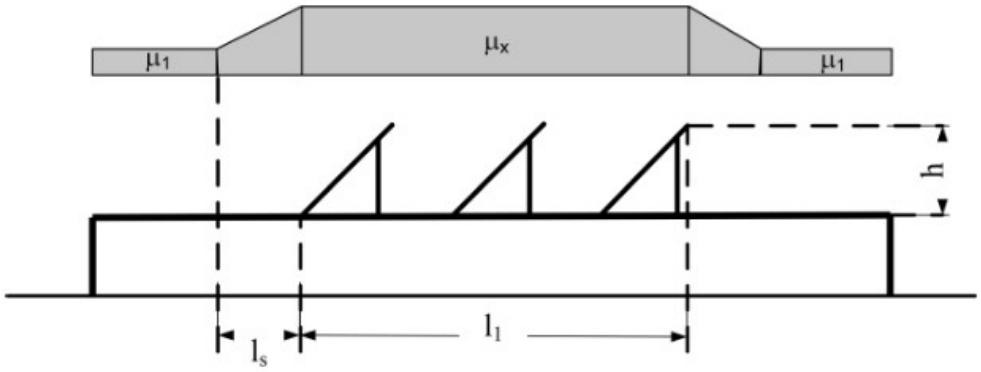

Figure 8- Shape Coefficient and Drift Length for Flat Roofs with PV Panels suggested by Formichi (2019)

CHAPTER 3

CONSTRUCTION OF PROPOSED GROUND SNOW LOAD MAP

3.1 ERA 5 Reanalysis Data

For last two decades, numerical weather prediction (NWP) models have provided invaluable achievements in the fields of climate research and weather forecast. The advances in computer technology make current atmospheric predictions more accurate and high resolution. The state of the art NWP models are used in climate research as well as operational weather forecast by several national or international research institutes like European Centre for Medium-Range Weather Forecast (ECMWF), National Centers for Environmental Prediction (NCEP), and National Aeronautics and Space Administration (NASA). The operational models are run typically 6/12 hours cycles which simulate future state of atmosphere and land surface up to several days or months by using the current state. On the other hand, reanalyzes dataset are obtained via data assimilation techniques which combining historical observation and model state.

After ERA-Interim where ERA refers to ECMWF Reanalysis, the fifth version reanalysis dataset named as ERA5 is released to public access. It is developed by Copernicus Climate Change Service which is an implantation of ECMWF and carried out with 4D-Var data assimilation procedure in ECMWF's Earth System Model IFS-CY41R2. The model consists of 137 hybrid sigma and pressure (model) levels up to upper mesosphere (0.01 hPa). The output of model has a 0.25^{o} resolution (approximately 31 km at mid-latitudes) and hourly temporal resolution (IFS DOCUMENTATION – Cy41r2, 2016).

As the most recent release of reanalyzes, ERA5 has already called attention of various researchers in terms of its accuracy on various meteorological parameters (Dieter, Elizabeth, & Claire , 2019), (Jaume , Llorenç , Verónica Torralba, Albert ,

& Francisco, 2019), (Clement , et al., 2018). Moreover, the latest global wind and solar resource maps have been carried out by using ERA5 dataset in dynamical downscaling procedure. Xiaoyong et al. (2019) compared different reanalysis datasets and concluded that ERA5 gives better results in terms of precipitation products.

3.2 Obtaining Annual Maximum Time Series for Era-5 Data

In order to constitute a ground snow load map snow depth or snow water equivalent measurements with at least 30 years of snow data are needed. This data is provided by historical data archive of meteorological stations. However, due to aforementioned problems in Section 2.1, instead of using station data ERA5 climate reanalysis data which is latest climate reanalysis produced by ECMWF is used.

First of all, ERA5 climate reanalysis data, "ERA5 hourly data on single levels from 1979 to present", is downloaded using ECMWF WebAPI. Since data is provided with global horizontal coverage, storage requirement is high and downloading process takes too long. To overcome this issue, location of Turkey is selected as geographic lat/long degrees using a Pyton script (Figure 9). Moreover, snow depth (sd) and snow density (rsn) variables are selected among various snow related variables provided. Data for all months and days between 1979 and 2018 at 07.00 UTC (Coordinated Universal Time) is downloaded in NetCDF format for the region in which Turkey is located.

Unit of the sd variable is meters of water equivalent thus it is actually snow water equivalent. Unit of rsn variable is kg/m^3 which is unit of snow density. By using this variables snow depth in meters can be obtained and be used for comparison with climate station data.

Finally, netCDF files are processed using MATLAB software and annual maxima time series (1979-2018) for snow depth and snow water equivalent belong to each grid point are obtained.

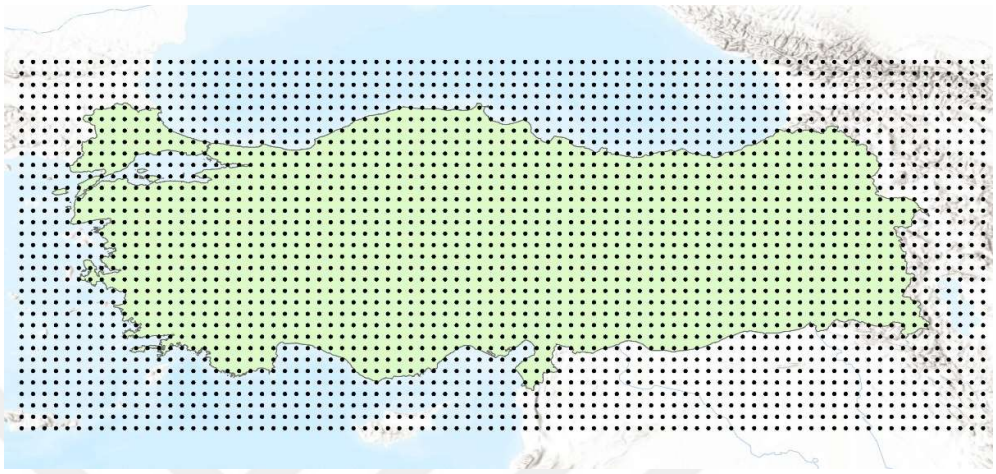

Figure 9- Grid points covering Turkey

3.3 Obtaining Annual Maximum Time Series for Climate Station Data

Daily measured parameters related with snow such as existing snow depth (cm), maximum snow depth (cm), snow water equivalent (mm) are obtained from 795 meteorological stations of TSMS measuring snow data are used for validation purpose. It is seen that for some time interval both existing snow depth and maximum snow depth parameters were measured however for some time interval only one of two parameters was measured. There is also discrepancy between two parameters such as daily existing snow depth being larger than daily maximum snow depth. To avoid losing valuable data and to obtain a daily snow depth time series with maximum number of available data, maximum of two parameters is selected as daily snow depth measurement. Afterwards, number of years of data available in concurrent time period with ERA 5 data, data after 1979, is calculated for each station. Stations having minimum 10 years of non-zero data of either maximum snow depth or snow water equivalent in concurrent time period are selected for first-step comparison purposes. Minimum 10 years of non-zero measurement in common time interval is available in 247 stations for snow depth and in 99 stations for water equivalent measurement.

For the first-step comparison, it is decided to compare annual maxima of snow depth and snow water equivalent measurements with annual maxima time series of ERA5 data belong to nearest grid point to subject station. Comparison of daily measurements with ERA5 snow data is not performed since snow measurements exist for only snowy days (no data for days with no snow or when snow depth is too small to measure) and it is observed that in many stations there were missing daily measurements. Moreover, annual maximum of data is needed for snow load calculations instead of daily maximum.

In order to compare measurements with ERA5 data, nearest grid point to each station is calculated using station and grid point coordinates. In cases where nearest grid point lies in the sea, the second nearest grid is chosen as nearest. Before making a comparison, TSMS data and ERA 5 data is plotted together for each station to have a general understanding about consistency of two datasets. For some stations, it is observed that general trend of two datasets are matching very well but it is apparent that there are missing data in TSMS dataset. In addition, for some stations, there were some TSMS data points violating general trend of data such as data points with very high values as can be seen in Figure 10 and Figure 11. This type of error seems to be caused by mistyping while transferring hand records kept on papers to digital media. After detecting erroneous data manually by eye for each station and removing from TSMS dataset; annual maximum data series belong to snow depth and snow water equivalent measurement are obtained.

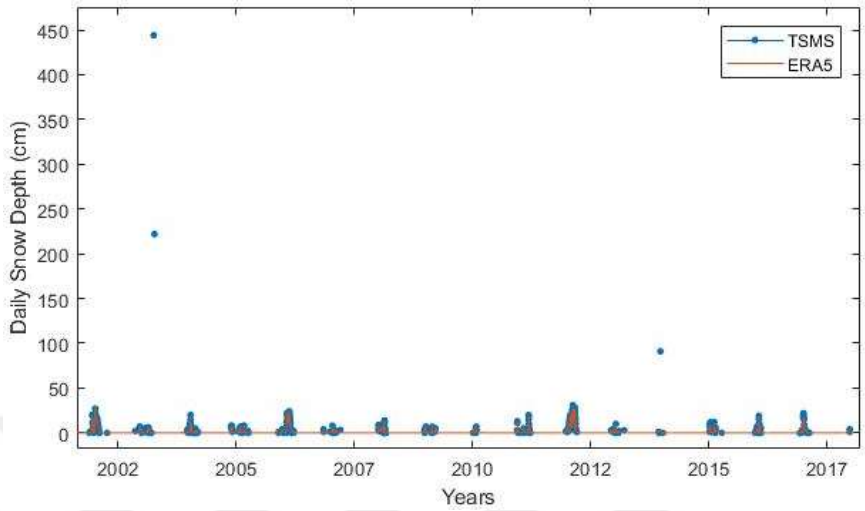

Figure 10- Station Data (Ankara-Esenboğa) Compared to ERA-5 Data (without error correction)

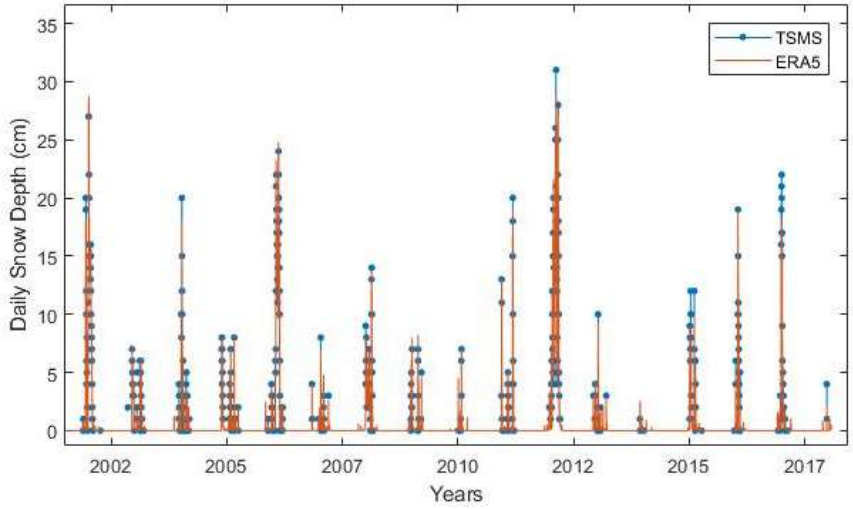

Figure 11- Station Data (Ankara-Esenboğa) Compared to ERA-5 Data (with error correction)

3.4 Comparison of Annual Maximum Time Series of ERA5 Data and Station Data

Annual maximum time series of snow depth and snow water equivalent parameters belong to TSMS measurements and ERA 5 are compared in order to have confidence on representativeness of ERA 5 snow products over Turkey. As stated by Tetzner, Thomas & Allen (2019), normalized bias (NBIAS), normalized mean absolute error (NMAE), and normalized root-mean-square error (NRMSE) are performance indicators used in reanalysis evaluation and Pearson's linear correlation (R) can be used to test statistical relationship between observed and reanalysis monthly mean values. In this study, instead of monthly means, annual maximum values are used to evaluate performance of ERA 5 reanalysis NBIAS, NMAE, NRMSE are calculated as follows:

$$NBIAS = \frac{1}{N}\sum_{i=1}^{N}\frac{x_{ERA\,5}(i) - x_{measurement}(i)}{y_{max}} \tag{14}$$

$$NMAE = \frac{1}{N}\sum_{i=1}^{N}\left|\frac{x_{ERA\,5}(i) - x_{measurement}(i)}{y_{max}}\right| \tag{15}$$

$$NRMSE = \sqrt{\left[\frac{1}{N}\sum_{i=1}^{N}\left(\frac{x_{ERA\,5}(i) - x_{measurement}(i)}{y_{max}}\right)^{2}\right]} \tag{16}$$

where $x_{ERA\,5}$ is annual maximum of each year of reanalysis, $x_{measurement}$ is annual maximum of each year TSMS measurements, y_{max} is maximum of annual maximum time series of TSMS measurements. Results of comparison is tabulated in Table A. 1 and Table A. 2 in Appendix where 'n' is number of comparable years. Figure 12 and Figure 13 show correlation between measured Snow Water Equivalent (SWE) and Snow Depth (SD) at station locations with nearest grid point.

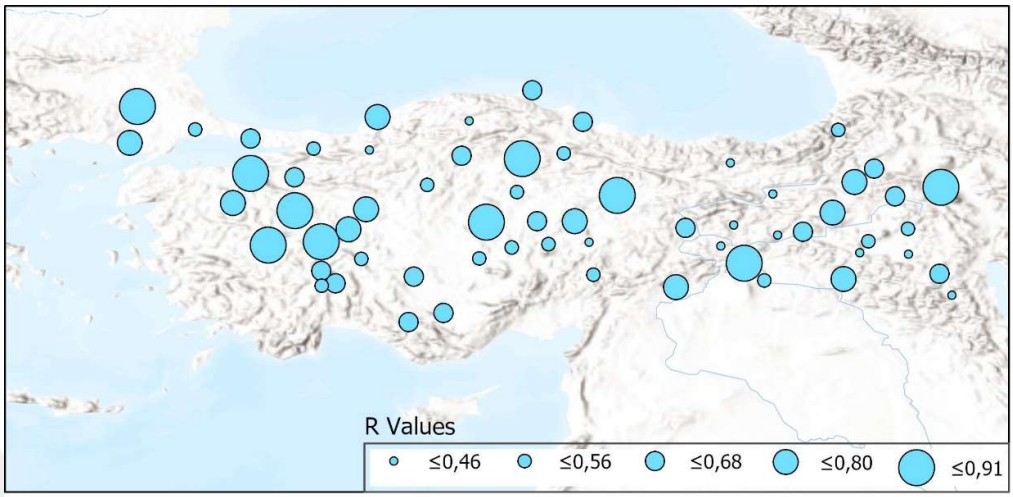

Figure 12- Correlation between measured SWE at station locations and nearest grid point

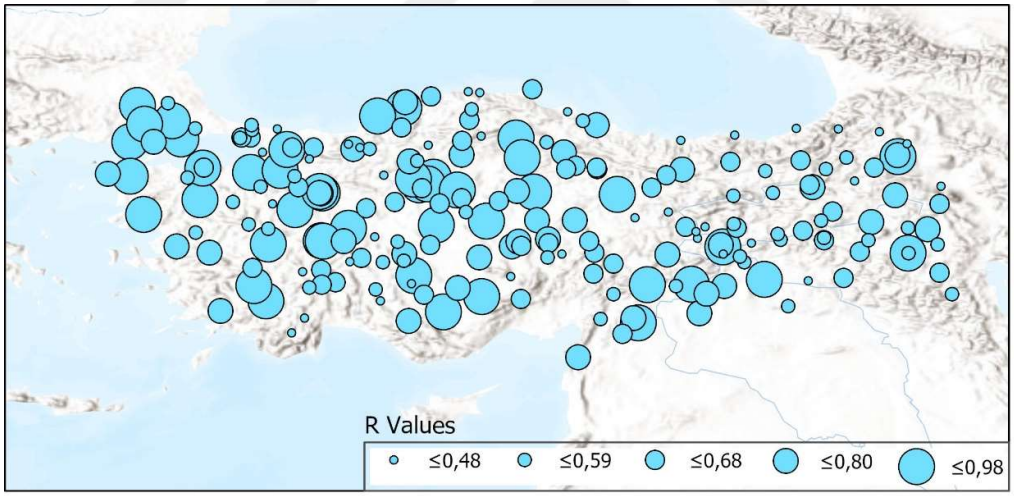

Figure 13- Correlation between measured SD at station locations and nearest grid point

According to performance indicators calculated for snow water equivalent data and sorting results according to R values (only statistically significant R values used, $p < 0.05$), ERA5 shows best performance for station located in Çorum (n=29, NBIAS=0.07, NMAE=0.09, NRMSE=0.11, R=0.92) as can be seen in Figure 14 and worst performance for station located in Tunceli (n=35, NBIAS=0.12, NMAE=0.24,

NRMSE=0.27, R=0.34) as can be seen in Figure 15. For 37 stations out of 99 stations where minimum 10 years of mutual time interval exists, there were no statistically significant correlation between ERA5 data and station measurements ($p>0.05$).

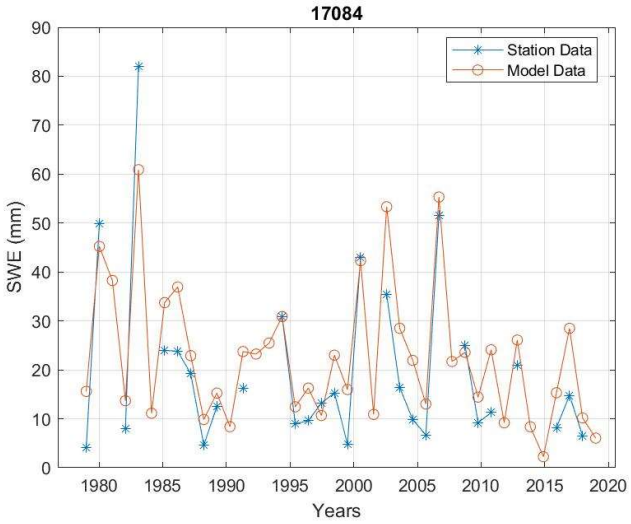

Figure 14- Annual Maximum SWE Time Series of Çorum Station (Station No=17084) and Model Data (R=0.92)

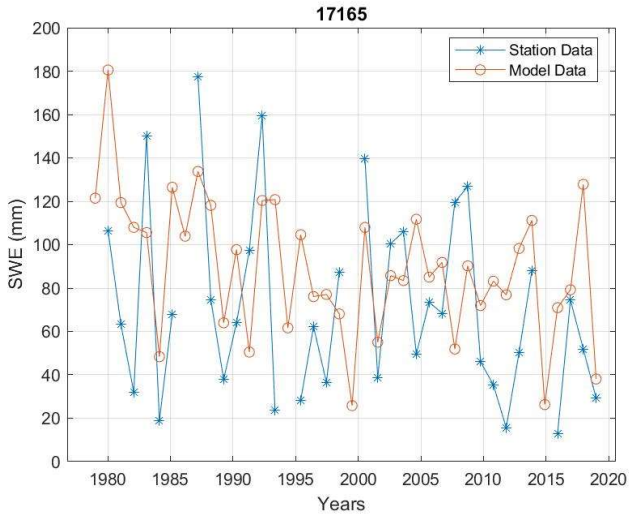

Figure 15- Annual Maximum SWE Time Series of Tunceli Station (Station No=17165) and Model Data (R=0.34)

According to performance indicators calculated for snow depth data and sorting results according to R values, ERA5 shows best performance for station located in Sivas (n=40, NBIAS=0.005, NMAE=0.024, NRMSE=0.046, R=0.98) and worst performance for station located in Sivas-Kangal (n=35, NBIAS=0.005, NMAE=0.19, NRMSE=0.25, R=0.35) as shown in Figure 16 and Figure 17. For 32 stations out of 247 stations where minimum 10 years of mutual time interval exists, there were no significant correlation between ERA5 data and station measurements ($p>0.05$).

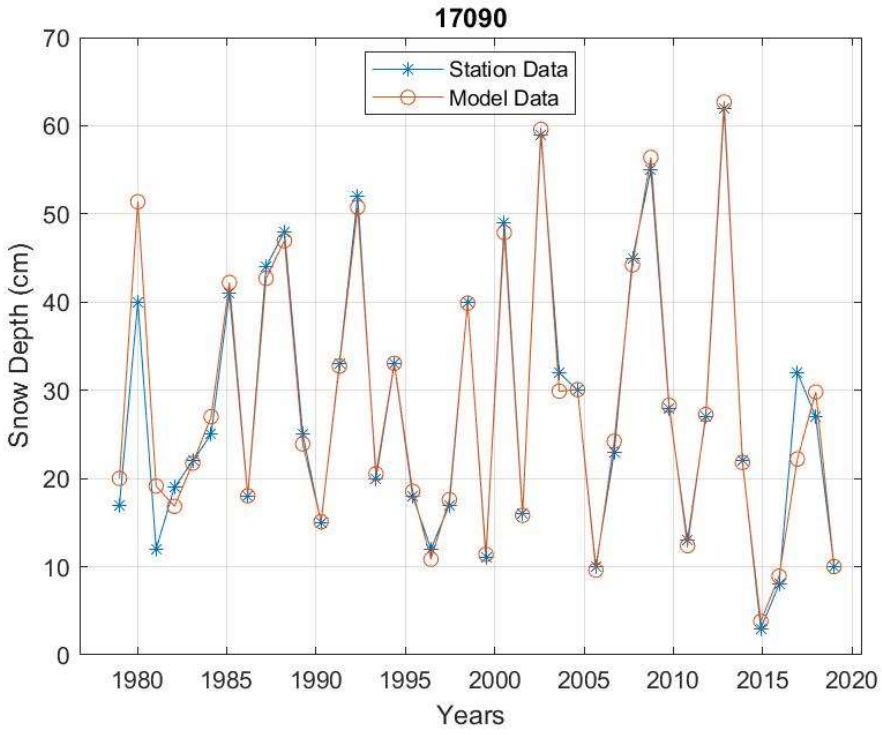

Figure 16- Annual Maximum SD Time Series of Sivas Station (Station No=17090) and Model Data (R=0.98)

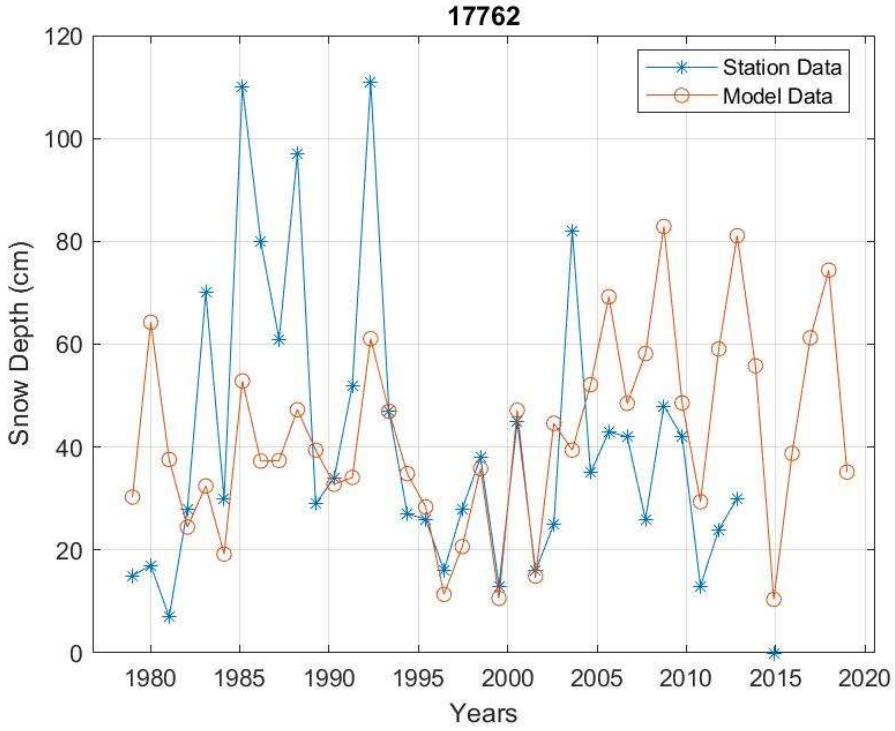

Figure 17- Annual Maximum SD Time Series of Sivas-Kangal Station (Station No=17762) and Model Data (R=0.35)

Obtained results show that correlation between ERA5 data and station measurements are higher for snow depth parameter (mean R=0.65) compared to snow water equivalent (mean R=0.62). For 46 of 62 stations (%74) having minimum 10 years of both snow depth and snow water equivalent measurements in concurrent time and having a statistically significant correlation for both parameters, correlation is higher for snow depth parameter. There are two stations (Van and Kars) having a correlation greater than 0.7 for snow depth parameter but shows no statistically significant correlation for snow water equivalent. Moreover, when only stations located in city centers and airports are considered, a higher correlation for both snow depth (R=0.71) and snow water equivalent (R=0.63) is observed.

In general low correlation between model and measurements is observed in eastern part of Black Sea Region, Eastern Anatolia Region and parts of Mediterranean

Region closer to Taurus Mountains. Possible reasons for this can be effect of elevation difference between closest grid point and station location or poor performance of ERA5 model in mountainous regions.

3.5 Determination of Ground Snow Loads at Grid Points

Firstly, annual maximum time series belong to snow water equivalent data (sd variable of ERA 5, given in meters of water equivalent) is converted to snow load. In order to construct a ground snow load map, characteristic snow load with 50-year MRI at grid points have to be determined using 40 years of annual maximum snow load data obtained in each grid point. Various probability distribution functions are proposed to simulate distribution of snow load as mentioned in Chapter 2.

Return period calculations require extrapolation of observed values since required return period generally exceeds observation interval. Thus, for calculation of snow loads with 50-year MRI using snow data records (with record length less than 50 years for most cases), it is important to approximate the behavior of the rare loads located in tail part of a probability distribution precisely. Tail is the portion of the probability distribution which is away from mean and there is no exact definition of tail indicating where it starts. Similar to DeBock, Liel, Harris, Ellingwood, & Torrents (2017), in this study tail fitting approach is used together with Lognormal distribution. Details of the method used is provided in Section 2.2.3.

An example of determination of ground snow load in a grid point using Lognormal tail fitting approach is explained in details. In this example, nearest grid point (Latitude=39.5, Longitude=30) to Kütahya station (Latitude=39.4171, Longitude= 29.9891) is used. Firstly, annual maximum ground snow data belong to 40 years from 1979 to 2018, x_1 to x_{40}, are sorted in ascending order and ranked starting from 1 to 40. Natural logarithm of x_i is calculated since they will be used in Lognormal probability plot. Then, empirical cumulative probability of each data point is calculated using equation (10) and a=0.375 as suggested by (Mehdi & Mehdi, 2011).

Finally, inverse cumulative distribution function, $z_i = \Phi^{-1}(p_i)$, is calculated for each p_i. To obtain Lognormal probability plot, $\ln(x_i)$ values are plotted against corresponding z_i values (Figure 18). Calculated values are given in Table 2.

Table 2- Determination of Lognormal Probability Plot

Rank	x_i	$\ln(x_i)$	p_i	z_i
1	0.019	-3.970	0.016	-2.156
2	0.059	-2.824	0.040	-1.746
3	0.099	-2.312	0.065	-1.512
4	0.119	-2.128	0.090	-1.340
5	0.128	-2.058	0.115	-1.201
6	0.128	-2.058	0.140	-1.081
7	0.129	-2.048	0.165	-0.976
8	0.131	-2.031	0.189	-0.880
9	0.135	-2.001	0.214	-0.792
10	0.135	-2.000	0.239	-0.709
11	0.154	-1.870	0.264	-0.631
12	0.176	-1.736	0.289	-0.557
13	0.206	-1.581	0.314	-0.485
14	0.228	-1.479	0.339	-0.417
15	0.230	-1.471	0.363	-0.350
16	0.271	-1.307	0.388	-0.284
17	0.275	-1.292	0.413	-0.220
18	0.276	-1.287	0.438	-0.156
19	0.286	-1.252	0.463	-0.094
20	0.290	-1.237	0.488	-0.031
21	0.300	-1.206	0.512	0.031
22	0.313	-1.162	0.537	0.094
23	0.332	-1.103	0.562	0.156
24	0.332	-1.103	0.587	0.220
25	0.356	-1.033	0.612	0.284
26	0.361	-1.020	0.637	0.350
27	0.367	-1.003	0.661	0.417
28	0.374	-0.984	0.686	0.485
29	0.393	-0.934	0.711	0.557
30	0.396	-0.926	0.736	0.631
31	0.397	-0.924	0.761	0.709
32	0.404	-0.905	0.786	0.792
33	0.448	-0.804	0.811	0.880

34	0.450	-0.798	0.835	0.976
35	0.543	-0.611	0.860	1.081
36	0.600	-0.510	0.885	1.201
37	0.634	-0.455	0.910	1.340
38	0.635	-0.453	0.935	1.512
39	0.843	-0.171	0.960	1.746
40	0.854	-0.158	0.984	2.156

After plotting rank-ordered data to probability plot, tail-fitting approach is used by fitting a least-squares-regression line to top 33% of data points (largest 13 values). Reciprocal of the slope of the fitted line ($R^2 = 0.95$), 0.6026, is standard deviation and x-intercept, -1.3162, is mean of the tail-fitted Lognormal distribution. Whereas, thick solid blue line in Figure 18 represents fitted line to tail portion, dashed blue line shows Lognormal fit to all data for comparison purpose. It is apparent that tail-fitted distribution does not fit well for low load values however it fits well for larger loads well with $R^2 = 0.95$.

Using tail-fitted Lognormal distribution with shape and location parameters μ=-1.3162 and σ=0.6026, ground snow load with 50-year MRI (0.02 probability of exceedance in on year) is calculated by equating inverse of cumulative distribution function of Lognormal distribution to 0.98. As a result, 50-year MRI ground snow load is calculated as 0.9243 kN/m^2.

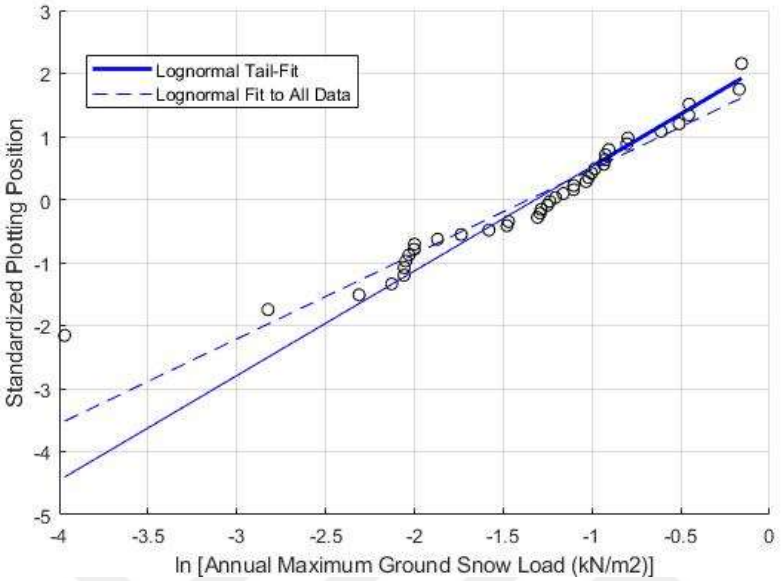

Figure 18- Lognormal Tail-Fit vs Lognormal Fit to All Data

For grid points with no annual maximum greater than 5 mm (approximately 0.05 kN/m^2), snow load is assumed as zero. Those grids generally lie in the sea. The procedure shown on example given above is used for all grid points and ground snow load values are determined using Lognormal tail-fitting approach. Mean of the correlation coefficients of fitted lines is found as 0.93. Ground snow loads obtained at grid points can be seen in Figure 19.

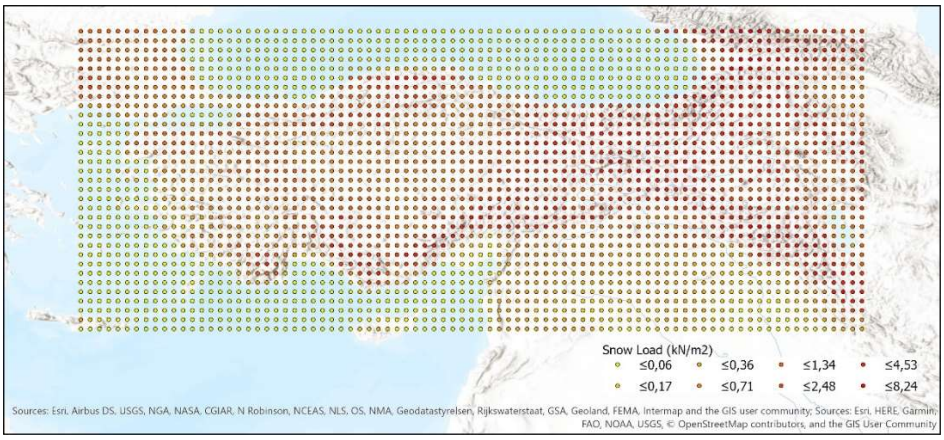

Figure 19- Ground Snow Values at Grid Points

Although 50 years is generally accepted mean recurrence interval for design snow loads in many codes and standards as well as EN-1991-1-3, it results in a probability of exceedance of 33% during the expected working life of 20 years for solar power plants. Moreover, for structures designed for an expected working life of 50 years, this probability increases to 64%. Since lightweight structures and roofs are vulnerable to snow loads compared to conventional building type of structures with lower snow load to dead load ratio, mean recurrence interval of 50 years for snow loads may results in unsafe design for lightweight structures and large span structures. For this reason, higher MRI is recommended for lightweight structures, for example in Chinese load code for the design of building structures (GB-50009 2012) 100-year return period value is recommended for design of lightweight structures.

In this study, a probability of exceedance of 10% over the design working life is chosen for both solar power plants with approximately 20 years of design working life and for conventional buildings with 50 years of working life. This results in a 190-year MRI and 475-year MRI design snow load respectively. Thus, ground snow loads with 190-year MRI and 475-year MRI are also calculated for grid points. Contour maps are constructed for snow loads with different MRI by interpolating grid point snow loads using co-kriging interpolation method and grid altitude is used as a covariate. Contour maps are shown in Figure 20, Figure 21, and Figure 22. Ratio of snow loads at grid points to 50-year MRI snow loads results in mean 1.44 for snow loads with 190-year MRI and 1.86 for snow loads with 475-year MRI.

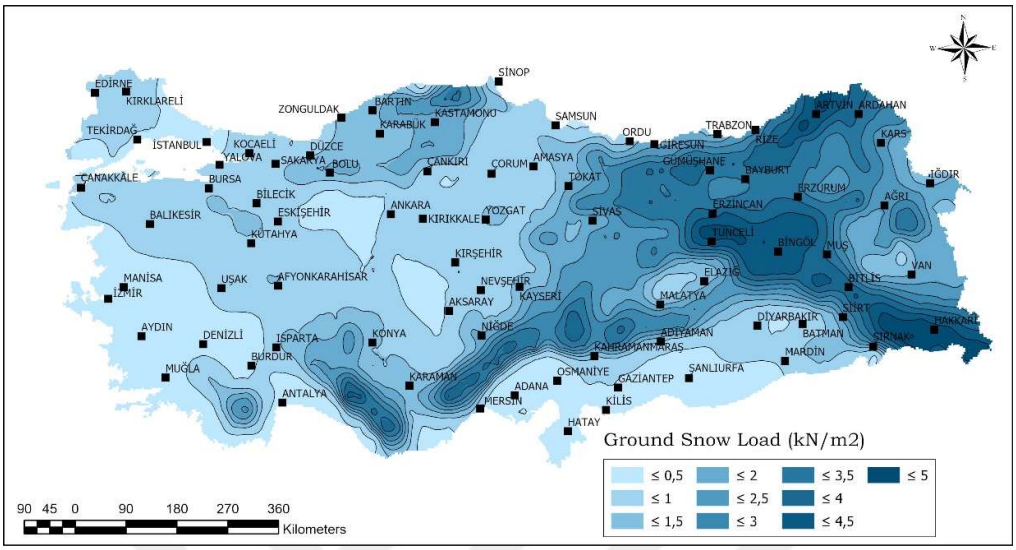

Figure 20- Ground Snow Load Contour Map for 50-year MRI

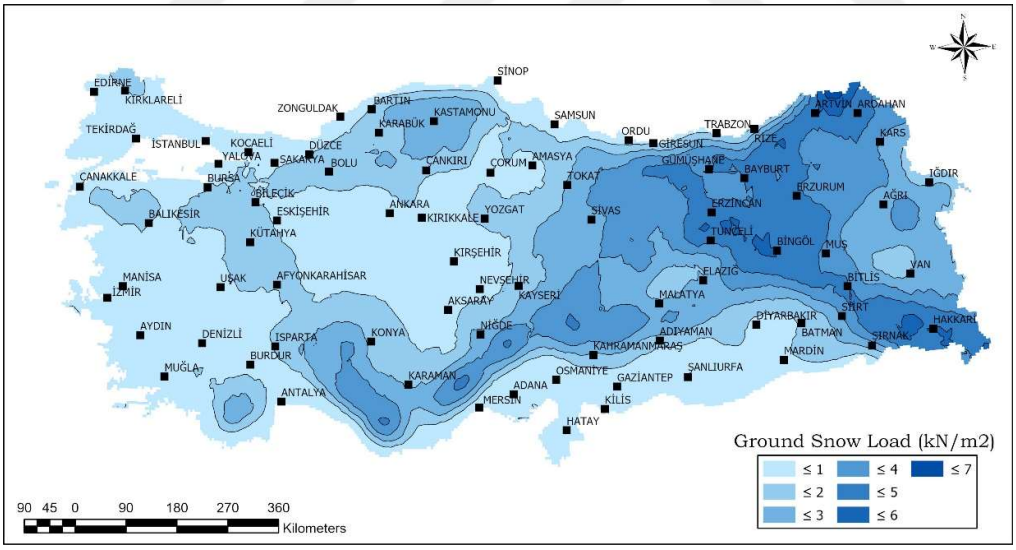

Figure 21- Ground Snow Load Contour Map for 190-year MRI

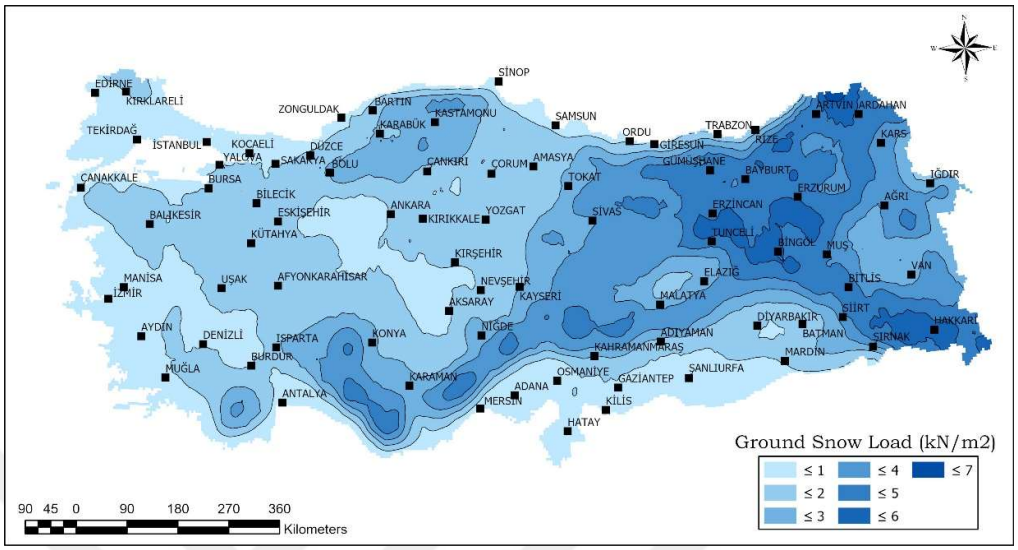

Figure 22- Ground Snow Load Contour Map for 475-year MRI

Standard deviation and coefficient of variation of 50-year MRI ground snow loads at grid points are calculated and mapped as shown in Figure 23 and Figure 24. Figure 23 shows that standard deviation of annual maximum snow loads are higher in regions with higher snow loads such as Eastern Black Sea Region, Eastern Anatolia Region and regions around Taurus Mountains. On the other hand, Figure 24 shows that coefficient of variation is smaller for those regions and higher coefficient of variation in regions located in sea side is probably due to irregular snowfall pattern observed in such places.

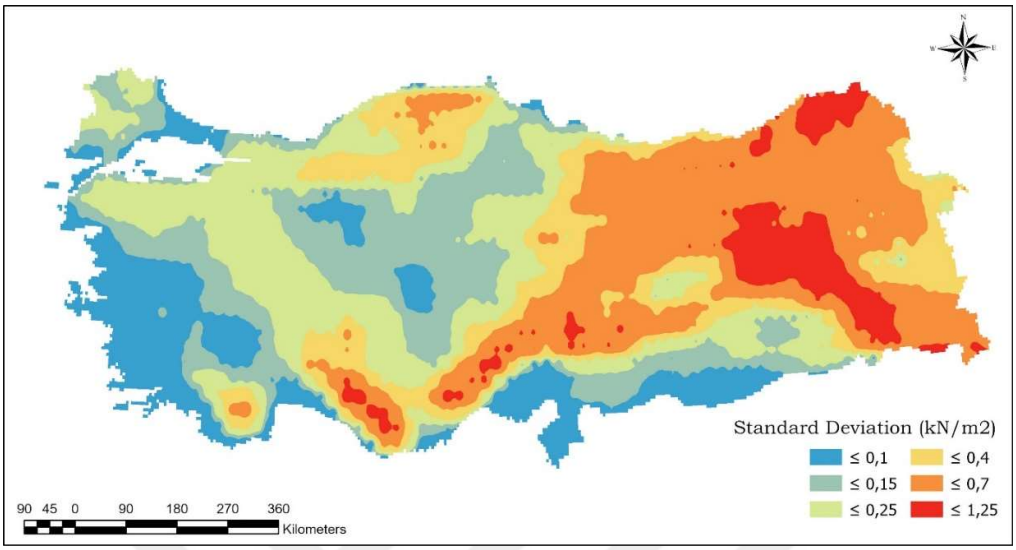

Figure 23- Standard Deviation of 50 Year MRI Snow Load Values

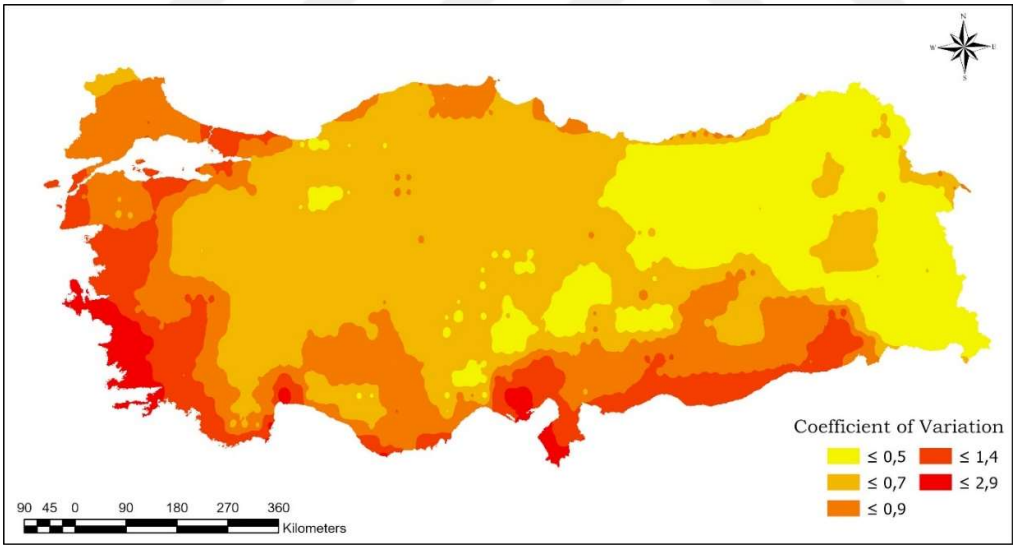

Figure 24- Coefficient of Variation for 50 Year MRI Snow Load Values

3.6 Determination of Ground Snow Loads at TSMS Stations

Ground snow loads at TSMS stations are determined in order to evaluate performance of ERA5 snow data. Similar to method used while calculating ground snow loads at grid points, Lognormal tail-fitting is used for TSMS stations. However, in order to calculate 50-year MRI snow loads, at least 30 years of snow data is needed according to studies in literature. There are 45 TSMS stations having more than 30 years of snow water equivalent data. For this comparison, instead of using data belong to concurrent time interval, all available observations are used. Snow water equivalent data is used for calculation of ground snow loads since they can be directly used without conversion using snow density needed for snow depth measurements. Since snow density cannot be calculated using a closed-formed formula, using snow depth data would bring additional uncertainty and effect results of comparison.

3.7 Downscaling of Gridded Snow Load Values

Since ERA5 data has 0.25º lat-lon grid resolution (approximately 31 km) a downscaling strategy is needed to obtain snow load values more precisely. In this study, similar to process used during development of Eurocode Snow Load Maps, altitude dependency of snow load is used for downscaling. Altitude function, in equation (11), provided in Snow Maps of many European countries, where a parabolic type of relationship (Central East, Alpine Region, Mediterranean Region, Iberian Peninsula, Greece) is found between altitude and snow load, is used for Turkey.

Firstly, land elevation data with 1 arc second (30m) resolution belong to Advanced Spaceborne Thermal Emission and Reflection Radiometer (ASTER) Global Digital Elevation Model Version 3 (GDEM 003) is used to find altitude of grid points. Grid points which stays in Turkey's borders are selected. Then, altitude is plotted against snow load and curve in the form of equation (11) is fitted. Best fitting curve shown

in Figure 25 results in b value equal to 1186. Using same b value for all grid points and snow load values calculated in previous section, parameter a for each grid point is calculated using equation (11).

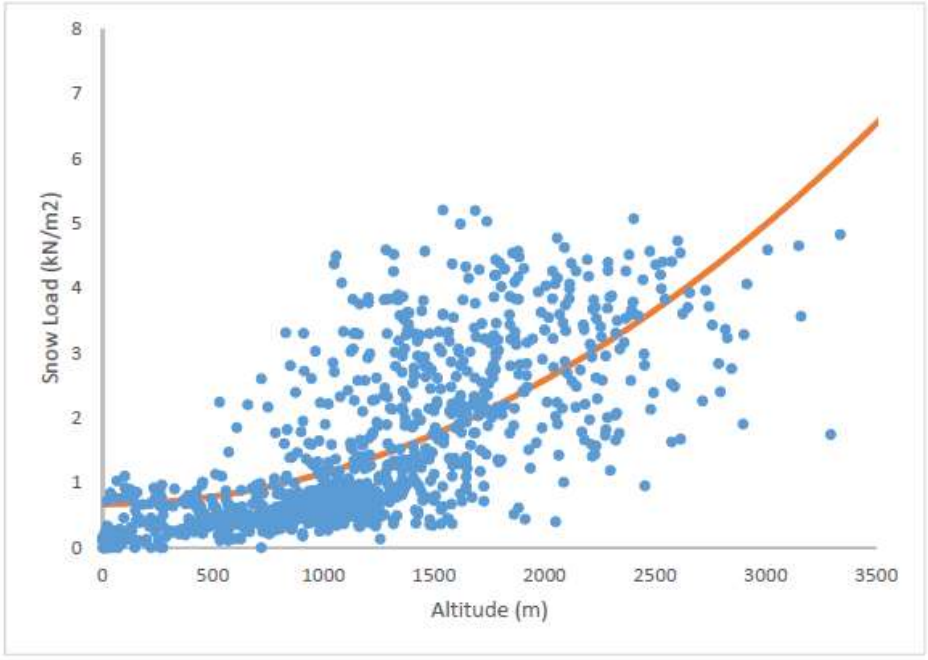

Figure 25- Best Fitting Altitude Function (a=0.6748, b=1186, R^2=0.46)

Using this equation, altitude dependency of snow load at grid points are eliminated thus parameter a represents snow load at sea level. Thereby, variation of snow load represented by parameter a among close grid points depend on other parameters leading local variations in snow load such as air temperature, solar radiation and wind exposure (Izumi, Nakamura, & Sacks, 1997). Since the effect of those factors are not easy to determine, assuming closer points show similar properties, Inverse Distance Weighing (IDW) interpolation method is used as a statistical downscaling method to determine parameter a at station locations. In IDW method, unknown values are calculated using weighted average of known values and weight given to each known point is inversely proportional to square of distance between known point and unknown point. Arcgis/Spatial Analyst tool box is used for IDW with

search radius of 12 nearest grid points and an output cell size of 0.001. Interpolated values are extracted for station locations from output raster.

3.8 Comparison of Ground Snow Loads

50-year MRI ground snow load values calculated at station locations are compared with loads calculated at nearest grid point and loads calculated using interpolated parameter a and equation (11). Results of the comparison is tabulated in Table A. 3 in Appendix. According to comparison of snow loads at station location with nearest grid point, for 26 of 45 stations snow loads calculated at nearest grid point are larger than snow loads calculated at station with mean percent error of 54.9%. For the rest, grid point values are less than station values with mean percent error of 28.6%. When snow loads at station location are compared with interpolated snow load values, for 21 of 45 stations interpolated snow loads are larger than snow loads calculated at station location with mean percent error of 44.43%. For the rest, grid point values are less than station values with mean percent error of 28.5%. Moreover, after interpolation for 26 stations absolute percent error decreased by mean 21% whereas for 19 stations absolute percent error increased by mean 11%. This results show that overestimation tendency of the model is higher. Moreover, it is seen that interpolation of snow load values to station points improves accuracy more for locations where ground snow loads are overestimated. In general, poorer results are obtained at regions with complex terrain such as Ardahan , Gümüşhane, and Giresun cities. This result is similar to results obtained by comparing annual maximum time series of grid points and station locations.

3.9 Mapping of Ground Snow Loads

Ground snow loads calculated at station locations need to be generalized to obtain snow load values in other locations. A regionalization procedure is needed to arrive at a geographic representation of results covering whole country.

Ground snow load value is influenced by many factors such as orography, presence of large lakes, distance to sea (macroscale effects); slope and contour of terrain, canopy, and crop density (mesoscale effects); surface roughness, presence of obstructions (microscale effects). All those parameters have to be considered when making a snow load map. However, it has been shown that altitude, air temperature, solar radiation, and wind exposure are very important parameters for local snow load variation (Izumi, Nakamura, & Sacks, 1997).

Since ERA5 data has 0.25° lat-lon grid resolution (approximately 31 km) a downscaling strategy is needed to obtain a high resolution map which represents local snow load variation. In order to construct a high resolution map, downscaling method shown in Section 3.7 is used and resolution is chosen as 0.001° lat-lon grid resolution (approximately 125 m). Parameter 'a' obtained in ERA5 grid points are interpolated using IDW interpolation method with search radius of 12 nearest grid points and an output cell size of 0.001. Thus a map representing variation of 'a' parameter is obtained as shown in Figure 26 . Then, ground snow load values are calculated using obtained 'a' parameter map and ASTER altitude data by substituting in equation (11) and ground snow load map is obtained as shown in Figure 27.

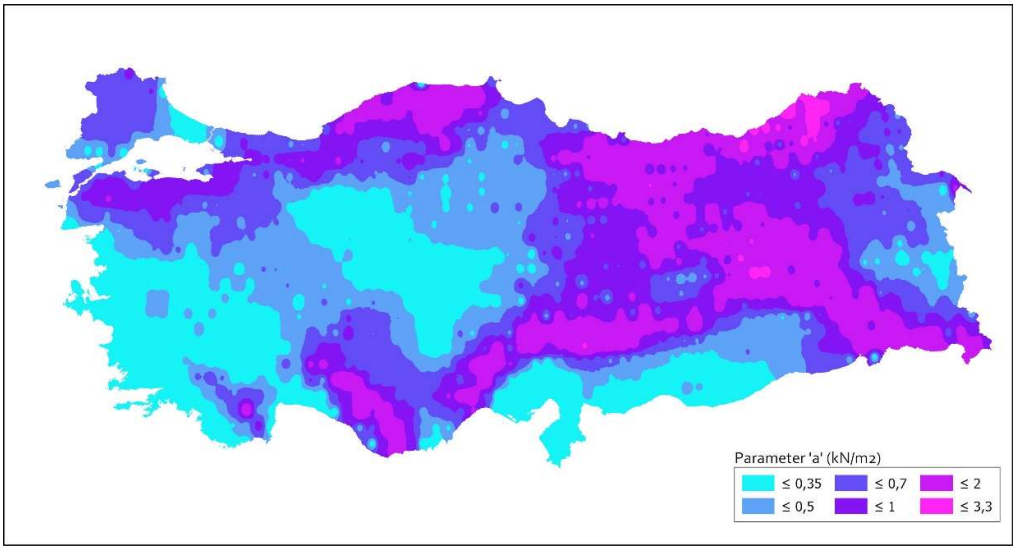

Figure 26- Mapped Values of Parameter 'a'

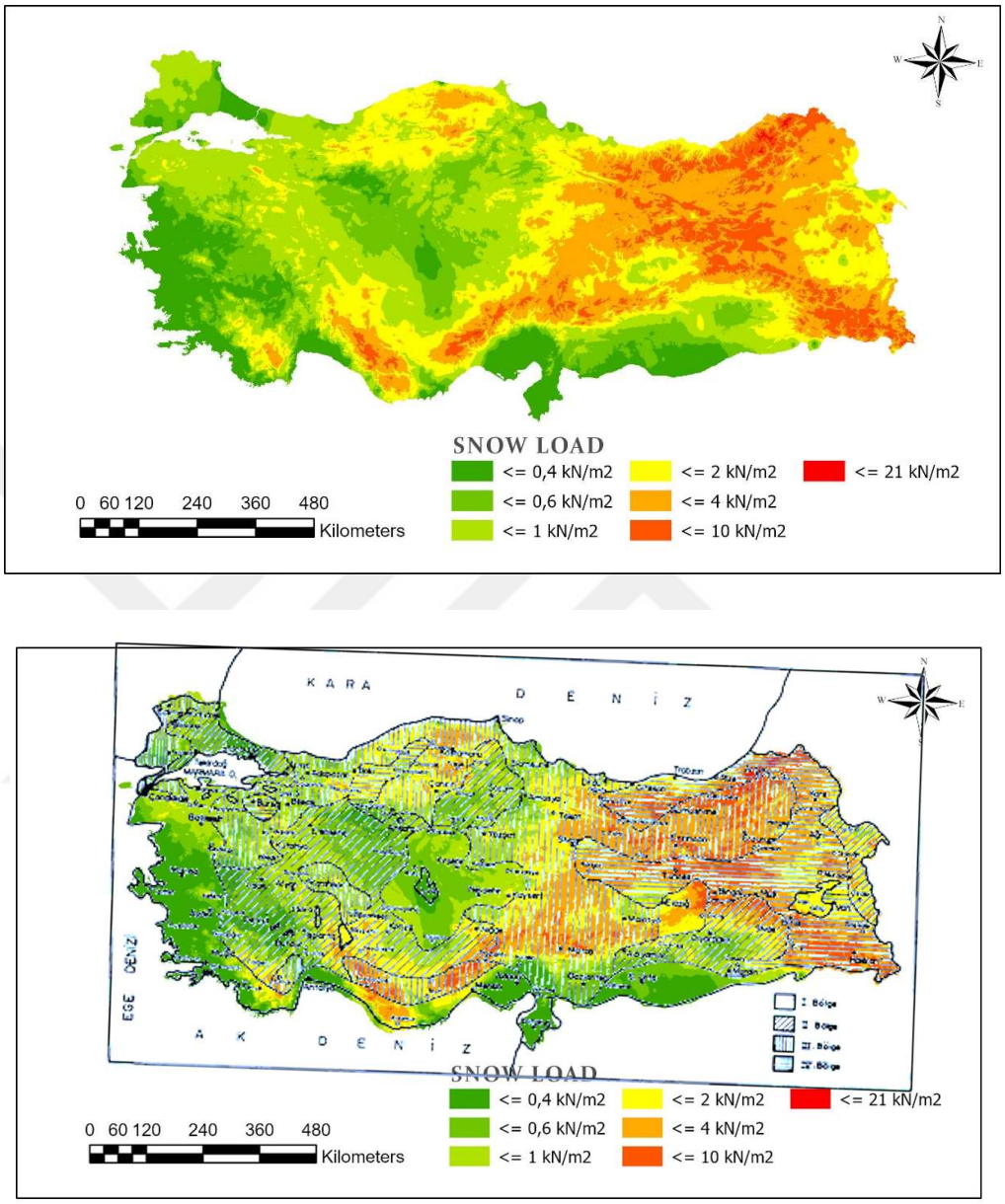

Figure 27- Mapped Values of Ground Snow Load and Overlapped Figures

3.10 Comparison of Proposed Map with TS498 Ground Snow Values

In TS 498 and National Annex of TS EN 1991-1-3, characteristic ground snow loads of Turkey presented by a map with 4 regions and a table showing load values as shown in Figure 28 and Table 3. In fact, in EN 1991-1-3 it is stated that provisions provided does not apply for sites with altitude above 1500m however it is also stated that treatment of snow loads for altitudes above 1500m can be provided in National Annex. However, in Turkish National Annex, it is stated that values provided for 1000 m should be increased 10% for sites with altitude above 1000m and 15% for sites with altitude above 1500m.

Ground snow load values taken from proposed map are compared with snow loads provided in Turkish provisions and snow loads obtained in 45 TSMS stations previously. TSMS stations used in comparison and snow loads calculated at station locations based on observations are shown in Figure 29. Tabulated results of comparison are provided in Table A. 4. In Figure 30, snow loads at TSMS stations are plotted against values taken from proposed map and TS498. Also a reference line is provided for comparison purpose by plotting loads at station locations against themselves. Then, a trend line is fitted for both proposed values and TS498 values. Correlation between observed values and proposed values (R=0.58) are higher than correlation between observed values and TS498 values (R=0.40). For 24 station locations, TS498 values are lower than observed with mean percent error of 33% and for 21 stations TS498 values are higher than observed with mean percent error of 51%.

Mean altitude of 45 TSMS stations used in comparison is 1038m. When overestimation and underestimation tendency of TS498 is investigated, it is seen that mean altitude of overestimated station locations is 923 m whereas mean altitude of underestimated station locations is 1138 m. This results show that TS498 gives unsafe snow load values for higher altitudes. On the other hand, overestimation of TS498 is probably due to minimum snow load value, 0.75kN/m^2, defined in TS498 for all regions.

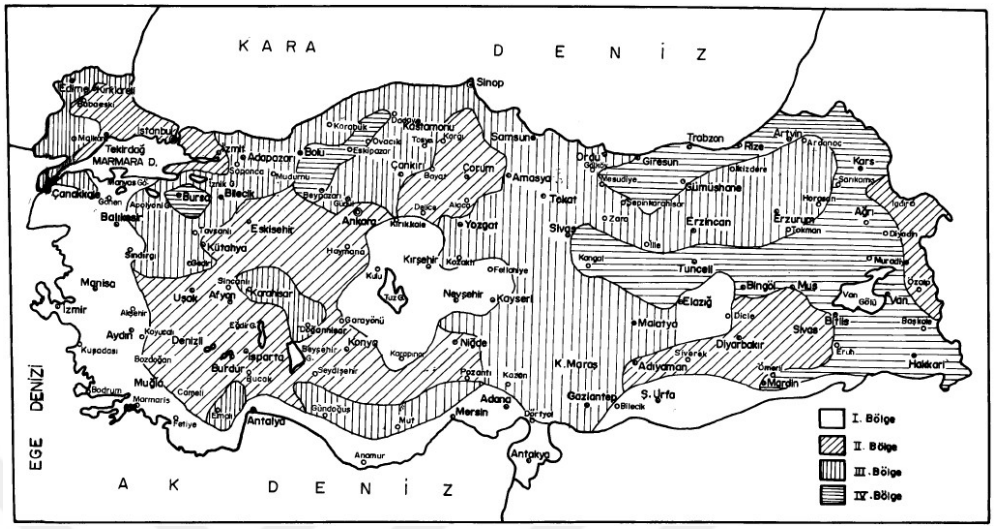

Figure 28- Ground Snow Load Map of Turkey in TS EN 1991-1-3

Table 3- Characteristic Ground Snow Loads kN/m^2 in TS EN 1991-1-3

Altitude (m)	Snow Regions			
	I	II	III	IV
≤200	0.75	0.75	0.75	0.75
300	0.75	0.75	0.75	0.80
400	0.75	0.75	0.75	0.80
500	0.75	0.75	0.75	0.85
600	0.75	0.75	0.80	0.90
700	0.75	0.75	0.85	0.95
800	0.80	0.85	1.25	1.40
900	0.80	0.95	1.30	1.50
1000	0.80	1.05	1.35	1.60
>1000	values belong to 1000m should be increased by 10% until 1500m and 15% above 1500m			
* Snow load should be taken as zero for places with no snowfall				

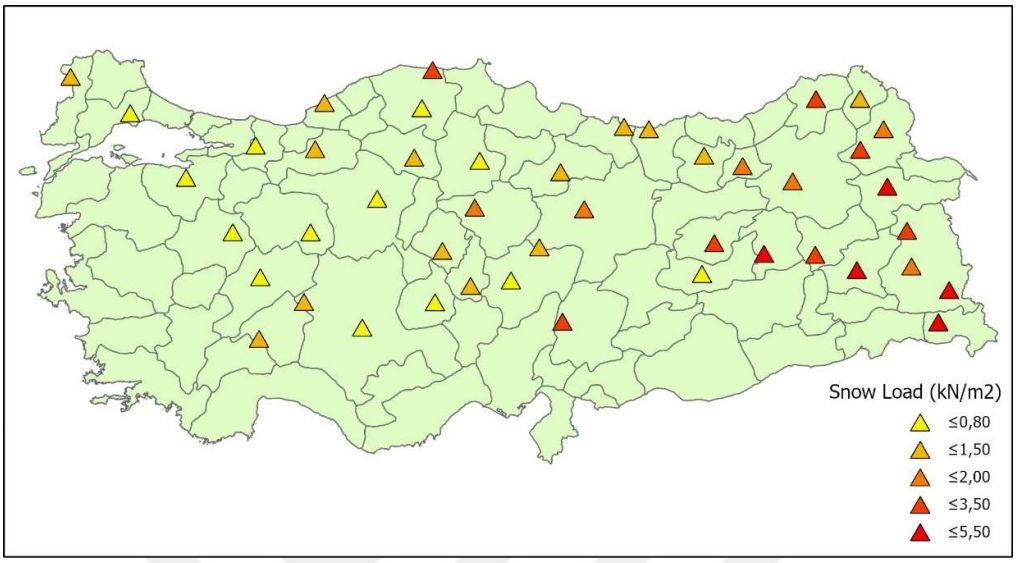

Figure 29- TSMS Stations Used in Comparison Shown on Turkey Map

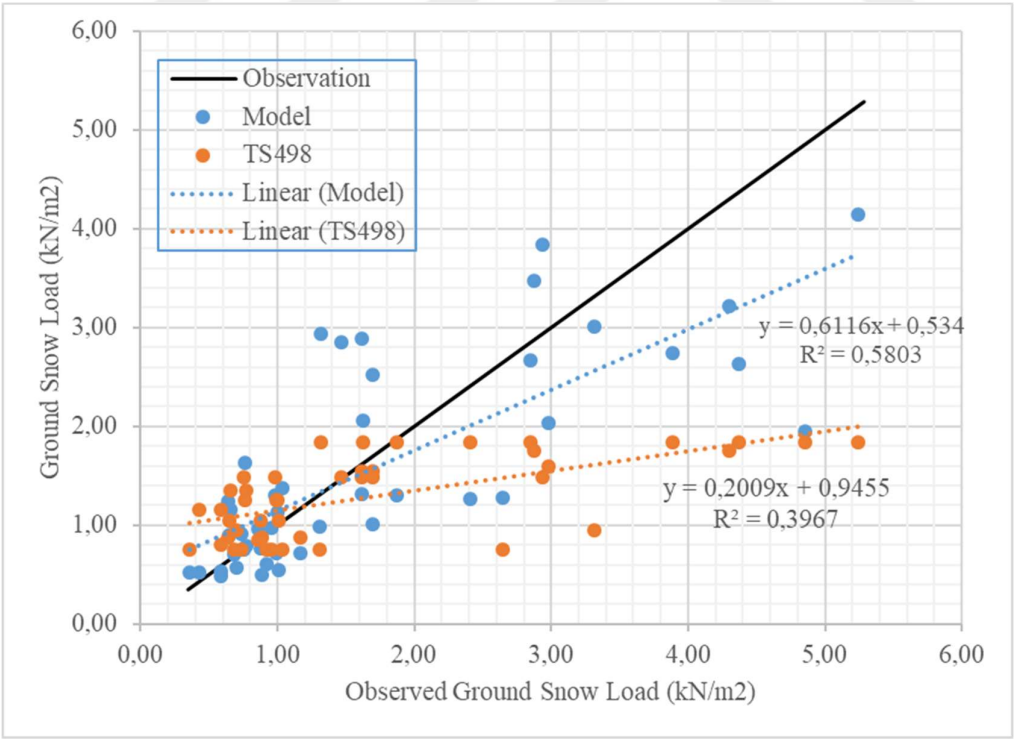

Figure 30- Comparison of Ground Snow Loads of TSMS Stations with Proposed Mapped Values (Model) and Values in Turkish Provisions (TS498)

When proposed map is compared with TS498, proposed map gives safer loads for 18 of 24 station locations where TS498 gives unsafe snow load values. Those stations are generally located at Black Sea and East Anatolian Regions. Conversely, there are 12 station locations mostly located in Central Anatolian Region where TS498 gives safer results than proposed map.

In addition to comparison made, in which results are verified using snow load values at TSMS stations, a comparison is made for 81 city centers in Turkey. Snow loads are taken from proposed map by using coordinates for city centers and from TS498 snow map. Tabulated results are shown in Table A. 5. According to obtained results, in 46 city centers snow loads provided in TS498 are higher than proposed values with maximum 86%, minimum %1, and mean 37% difference. On the other hand, for 32 city centers, TS498 snow loads are lower than proposed values with maximum 227%, minimum %8, and mean 67% difference. Difference is also represented in Figure 31. Shades of green in the figure shows city centers where TS498 provides higher snow loads whereas shades of red shows the opposite. It is observed from the figure that proposed snow loads are higher than provided by TS498 for city centers with higher altitude (mean altitude of places shown in shades of red is 905 m whereas mean altitude of places shown in shades of green is 621). This results are similar to results obtained in previous comparison validated using snow loads calculated at TSMS stations. Moreover, in other studies on Turkish snow loads conducted by Özgen (2007) and Durmaz & Daloğlu (2014) similar results were found. According to these studies, TS498 snow load values were found unsafe for about 30% of city centers which are mostly located in Eastern Black Sea, Eastern Anatolia, and coastal parts of Black Sea Regions. In addition, for 71.7% of city centers (43 out of 60) evaluated in study of Durmaz & Daloğlu (2014), mostly located in Aegean, Marmara, and Central Anatolian Regions, TS498 snow loads were found uneconomical.

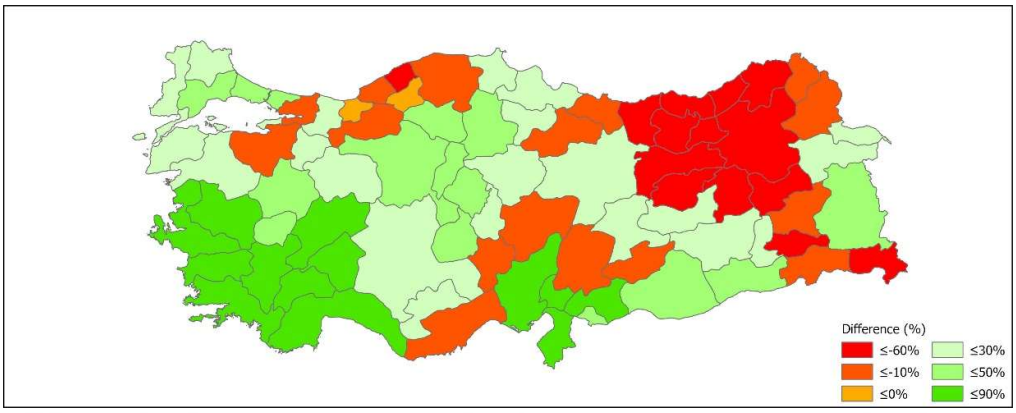

Figure 31- Percent Difference between TS498 Values and Proposed Values for City Centers

3.11 Change Trend in Snow Loads

Change trend in snow loads over the 40 years with available ERA-5 data (1979-2018) is calculated for each grid point. In order to determine the trend, best fitting line to annual maximums of 40 years of data is determined using least square regression. Slope of the fitted line gives the change in snow load in one year for the grid point analyzed. Slope of the fitted line is multiplied by 40 in order to obtain change trend in annual maximum snow load over the course of 40 years. Obtained values are shown in Figure 32. Negative values on the map indicates a decrease trend in snow loads conversely a positive value means an increase trend in snow loads in 40 years. As can be seen from the figure, in general a decrease trend is observed in regions with higher snow loads and an increase trend is observed for regions with lower snow loads. However, there are regions showing a different trend from places in close proximity.

Decrease trend in snow loads is expected in general as a result of increase in mean temperature due to global warming. However, climate change has many aspects and its effect differs from region to region depending on orographic conditions which can cause a decrease in average snow height over larger regions but an increase in height of local snowfalls. (Croce, et al., 2018).

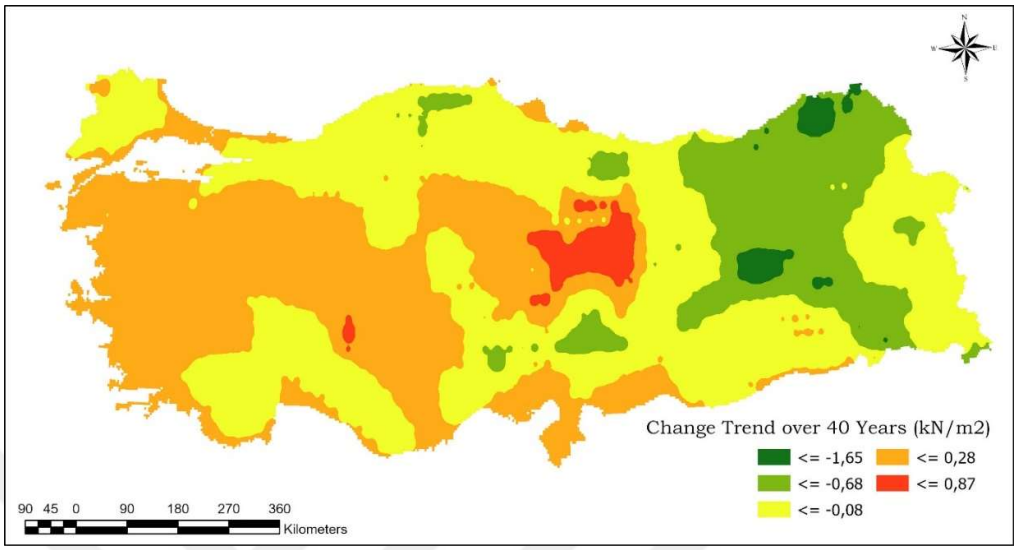

Figure 32- Change Trend in Annual Maximum Snow Load Over the Course of 40 years (1979-2018)

CHAPTER 4

RECOMMENDATIONS ON PREVENTION OF SNOW DAMAGE OBSERVED IN SOLAR POWER PLANTS

4.1 Typical PV Mounting Structures Used in Turkey

PV arrays are mounted on frames which serve as a structural support and keep panels in optimum tilt angle. In Turkey, PV panel mounting structures in solar power plants are generally constructed with aluminum or cold-formed steel profiles. Frame is constituted by one or two columns, one beam, and purlins carrying PV panels. Typical view of a fixed angle PV mounting structure with two columns is shown in Figure 33. Columns are generally driven into soil by man-power or Hydraulic Pile-Driving Machine. Driven columns are preferred since it is a low-cost solution and can quickly be implemented compared to reinforced concrete foundations.

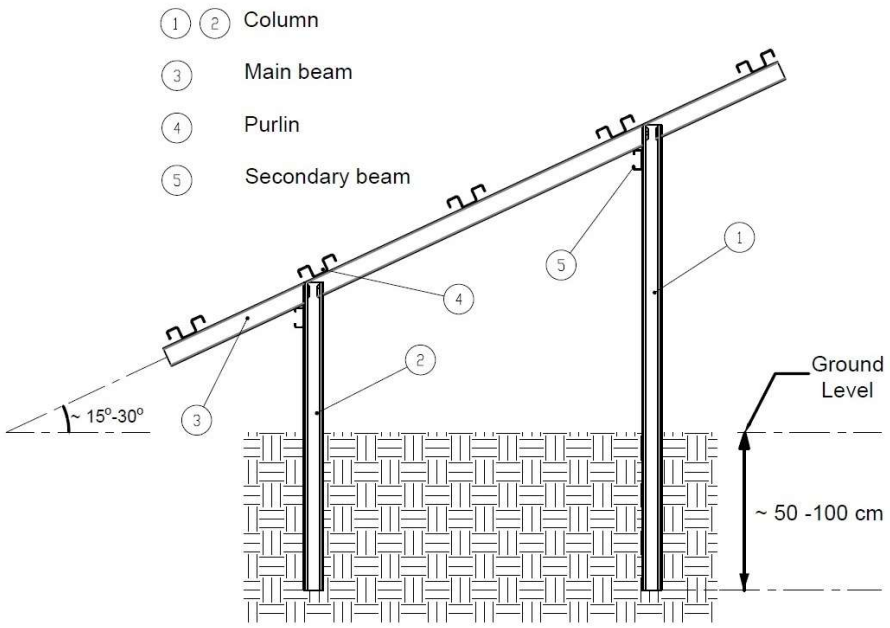

Figure 33- Typical View of PV Mounting Structures

4.2 Observed Snow Damage in Solar Power Plants

Snow damage was observed in mountainous regions of Konya, Kayseri, and Kahramanmaraş cities. Possible reasons of damage were reported as lack of representativeness of ground snow loads provided in TS498 for locations where snow damage occurred and errors made in structural design and assembly stages Ekol Loss Adjusting (2018) .

When structural design reports of damaged PV mounting structures are investigated, for most cases it is seen that snow load regions defined in TS498 were not properly selected considering location of the structure. In addition, for some cases ground snow load on plant location were higher than proposed by TS498. Ground snow load is highly correlated with altitude. Damaged sites are located in higher altitudes compared to city centers of site locations. According to results obtained in this study and similar studies in literature, snow loads provided by TS498 were found to be lower than actual for city centers in higher altitudes and locations where location considered has a higher altitude than average altitude of the city.

Moreover, geometry of PV mounting structures allows snow drift due to a similar behavior observed in snow fences. PV arrays located in foothills of mountains constitute an aerodynamic shade region for windblown snow. Since the amount of drifting snow depends on amount of driftable snow and wind, wind blowing from mountain top carries snow particles towards the mounting structures and creates the suitable condition for snow drift. Snow drift between successive rows of PV arrays can be seen in Figure 34, Figure 35, and Figure 36. In addition, Figure 34 shows that snow depth on the panels are much higher than snow on obstruction marked in red circle. In structural design reports of damaged structures, it is observed that effect of snow drift was not considered in snow load calculations of damaged structures.

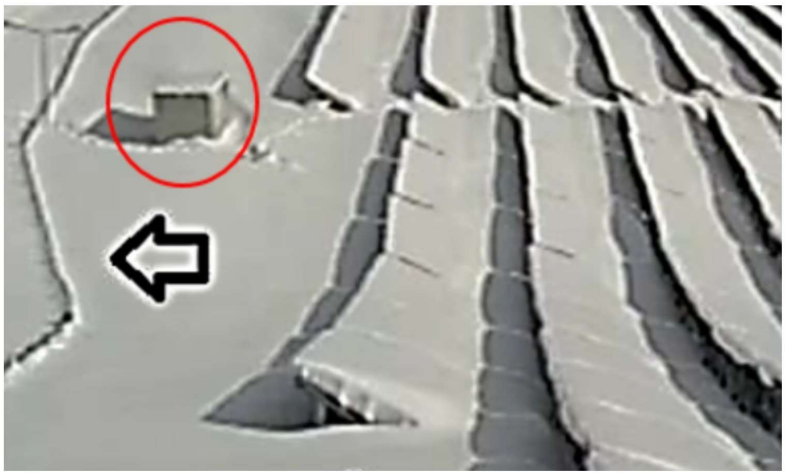

Figure 34- Snow Accumulation on PV Panels-1

Figure 35- Snow Accumulation on PV Panels-2

Figure 36- Snow Accumulation on PV Panels-3

Inspection on damaged structures revealed that main beams of structural system of mounting structures were deformed due to lateral torsional buckling as can be seen in Figure 37 and Figure 38. Lateral torsional buckling is a buckling phenomenon resulting in both lateral displacement and twisting and it is observed in sections with unrestrained compression flange. In a typical PV mounting structure main beams are cold-formed thin-walled channel sections which have low torsional rigidity and open configuration. In addition, load application point and the shear center of the section does not coincide since loads carried by purlins are transferred to main beam along center of gravity of the section rather than its shear center. These properties of channel sections increase tendency of lateral torsional buckling. When structural design reports are examined, it is seen that effect of torsion acting on main beams due to eccentric loading was not taken into consideration in design calculations. Damaged beams are modeled using SAP2000 software and lateral torsional buckling is observed in modelled structure as shown Figure 39 as expected.

Figure 37- Damaged Main Beam-1

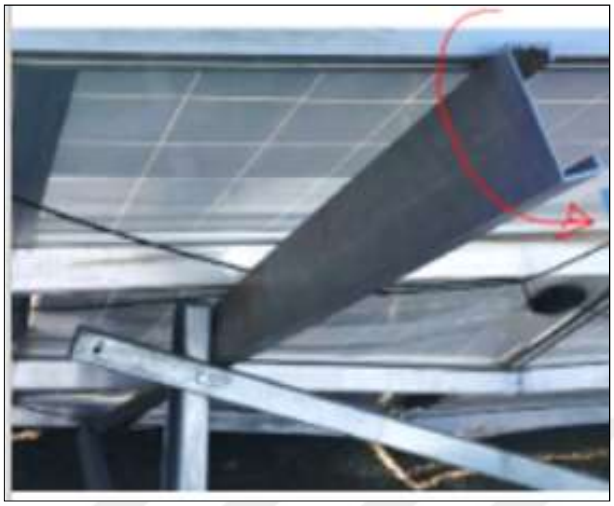

Figure 38- Damaged Main Beam-2

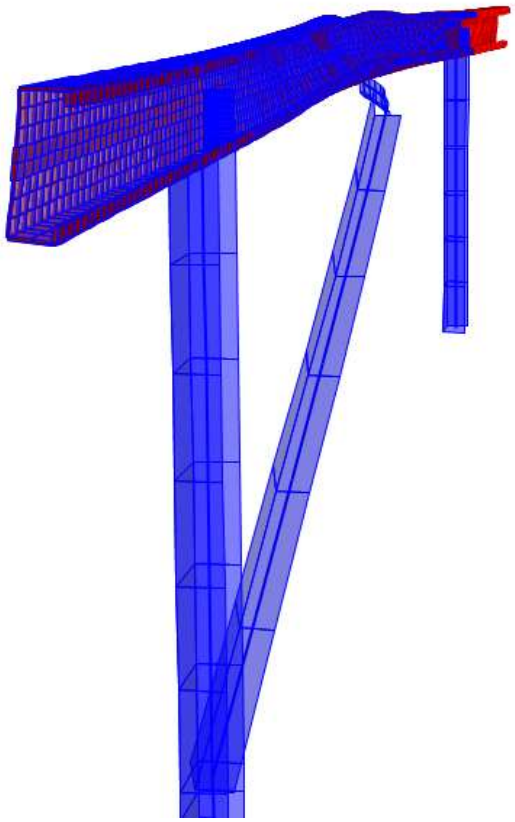

Figure 39- Buckling of Main Beam under Dead Load+Snow Load

In addition to errors made in structural design stage, several errors made in assembly stage caused damage in PV mounting structures. Some of the errors observed can be summarized as follows:

- Using unsymmetrical sections such as C channels where load is not acting at the shear center.
- Diagonal members to beam connections and beam to column connection being highly eccentric causing additional rotational effects on structural members.
- Failure to check bearing load capacity of connections.
- Not using profile thicknesses or dimensions determined in structural analysis stage
- Using screws instead of bolts in connections
- Using driven columns instead of concrete foundations without fully considering soil properties in the field and insufficient depth penetration to soil.
- Not considering additional snow because of heights above 1000m and 1500m
- Not considering snow accumulation because of wind and panels being too close to the ground.
- Various workmanship mistakes.

4.3 Recommendations

Considering reasons of snow damage mentioned in previous section, recommendations are given on ground snow loads, snow load shape coefficients, and structural system regarding lateral torsional buckling.

Determination ground snow loads requires data collection for at least 30 years in order to confidently determine 50-year MRI snow loads. Thus, there are two options to determine snow loads. One option is using snow loads provided by TS498 and the other option is to calculate snow loads using measurements of nearest meteorological

station if available. However, as mentioned previously snow loads provided by TS498 may not represent the site characteristics and structural geometrical properties especially if site elevation is higher than 1000 m and site has a concave up geological formation suitable for snow accumulation by wind. In addition, even if there is an available station close to plant location, many meteorological stations measure snow depth instead of snow water equivalent which can be converted into snow load directly. Another problem about meteorological measurements are “missing data”, “relocation of station”, and various uncertainties in the measurement of snow parameters. Thus, snow map provided in this study may be used in places where proposed values are higher than given by TS498.

Effect of snow drift is taken into consideration in snow load calculations in design codes. In TS EN 1991-1-3, two load arrangements are defined for undrifted and drifted snow and snow load shape coefficients are given for the two load arrangements depending on shape of the roof. There is no provision in TS EN 1991-1-3 providing guidance for snow loads acting on PV mounting structures in solar power plants. However, PV mounting structures can be interpreted as a multi-span roof and drifting load case defined in provisions can be used to determine snow load shape coefficients. In addition, model proposed by Formichi (2019) for about snow load distribution on flat roofs with PV arrays can be interpreted for PV mounting structures.

Since lateral torsional buckling is observed in sections with unrestrained compression flange, restraining compression flange of channel beams with braces will prevent lateral torsional buckling.

Shear and torsion related shear in open channels are often times not correctly calculated by the designers. A direct calculation from SAP2000 or similar software is taken directly without questioning. Professional engineers that are experienced in SPP design would be preferred for the design.

CHAPTER 5

CONCLUSIONS AND FUTURE WORK

In this study, a new ground snow load map is proposed for Turkey based on ERA5 Climate Reanalysis data and recommendations are made in order to prevent snow damage in solar power plants (SPP). Focus is given on examination of ground snow loads since it is important to approximate snow loads accurately for safe design of especially lightweight structures and roofs. Additional recommendations are extended for Mean Recurrence Interval (MRI), load distribution, connections, and section selection of structural members. Main findings and conclusions of this study are as follows:

- Snow loads provided in TS498 are unsafe for city centers with high altitude generally located in Eastern Black Sea and Eastern Anatolia Regions. In addition, in many locations with altitude above 1500 m, %15 increase in snow loads proposed in TS498 results in a maximum 1.84 kN/m^2 snow load, which is smaller than the actual increase caused by increasing altitude as obtained in this study. On the other hand, minimum snow load defined for all regions, 0.75kN/m2 results in uneconomical results for many cities, which are generally located in south and southwestern Turkey.
- Snow loads derived from proposed map in this study shows a better correlation than TS498 when comparison is made by using TSMS stations, which has minimum 30 years of snow water equivalent. It is seen that proposed loads are lower compared to TS498 generally in places with moderate climate conditions and where snow load is found as 0.75kN/m^2 using current snow load map. However, proposed snow loads values better represent snow load variations in higher altitudes when compared with the

current snow load map in use. Although much better than current map, the proposed snow load map still has some shortcomings: these are, a) relatively low performance in places with complex terrain and b) wind induced snow accumulation has to be considered separately. Although loads obtained using proposed map shows better correlation with observations as compared to TS498, values are still not as close as wanted. Possible reason of this drawback can be insufficiency of grid resolution of ERA5 data (approximately 31 km) and interpolation. Determining snow loads in places with complex terrain where altitude has ups and downs requires higher resolution to detect changes in snow load. As a result, it is recommended to use TS498 for places where proposed map gives lower loads to be on the safe side and for the opposite case, if there is no available/sufficient meteorological measurement, proposed map can be used.

- For structures vulnerable to snow loads due to higher snow load to dead load ratio compared to conventional building type structures, 50-year MRI design snow loads may result in unsafe design. The probability of failure (PoF) is obtained as 33% for structures with 20-year service life and 64% PoF for structures with 50-year design working life. In order to achieve the common 10% PoF, snow load MRI of 190 years need to be considered for 20 years of service life and 475 year MRI need to be considered for 50 years of service life. The current snow load map with 50-year MRI, annual probability of exceedance of 0.02, must be scaled with 1.44 for snow loads with 190-year MRI and 1.86 for snow loads with 475-year MRI.
- There is a decrease trend over 40 years (1979-2018) in ground snow loads for many locations in Turkey. This observation is probably due to the increase in mean temperature by climate change; however, it is also possible to observe an increase in snow height due to local orographic characteristics. Location with relatively small amounts of snow load showed an increasing trend over the course of last 40 years; increase trend primarily in Aegean

region and central Anatolia, highest increase trend being in Sivas. Largest descending trend is in Bingol and Artvin.

- Largest Coefficient of Variation (COV) in snow load based on 50-year MRI is obtained at the Marmara, Aegean, and Mediterranean coastal zones including Hatay and Syrian border all the way to Şırnak. The warm climate associated with these regions cause unpredictable snow precipitation causing larger COV; however, relatively small median. Standard deviation is much smaller in magnitude at the regions of large COV and doesn't impose a large threat. Largest standard deviation is seen in eastern Blacksea region, eastern Anatolia, and Taurus mountains higher elevations.
- As a result of literature review made as a part of this study, no provision or recommendation is found regarding snow load shape coefficients to be used in design of PV mounting structures. All of studies and provisions on snow loads on PV panels are focused on effect of existence of rooftop PV arrays on snow accumulation and distribution on roofs. Thus, recommendations are made by making inference with similar structures. For PV arrays having a row spacing less than two times the height of solar panels, the snow may be considered as completely filling the solar panels up to the highest point of solar panels. Any snow underneath the panels are ignored and not considered to load carrying mechanism.
- When damaged structures are observed, it is seen that there are errors made in structural design, workmanship, connections, and cross section thickness selection stages. Usage of braces between main beams in order to prevent lateral torsional buckling is recommended and problematic issues related with assembly stages are mentioned. Connections between the PV panels and structural load carrying members should be stable and not get lose over time.

For future investigations, the following studies may be conducted on the subject of this thesis:

- Since climate reanalysis data is published with better atmospheric models and higher resolutions day by day, using a higher resolution data available at time of investigation can lead to overcome some of the drawbacks of current proposed map.
- Dynamic downscaling methodologies with use of Weather Research and Forecast (WRF) models, in which physical principles are used, may be used instead of statistical downscaling methods (as IDW interpolation method used in this study).
- An online database of snow load using GPS coordinates will be prepared as a part of this thesis.
- It is seen that there is a need for studies on snow relocation and built-up observed in solar power plants in order to find snow load shape coefficients.

REFERENCES

Chitturi, S., Sharma, E., & Elmenreich, W. (2018). Efficiency of Photovoltaic Systems in Mountainous Areas. *2018 IEEE International Energy Conference (ENERGYCON).* Limassol, Cyprus: Institute of Electrical and Electronics Engineers.

Copernicus Climate Change Service (CS3). (2017). ERA5: Fifth generation of ECMWF atmospheric reanalyses of the global climate. Copernicus Climate Change Service Climate Data Store (CDS). Retrieved 2019

Council, I. C. (2012). *International Building Code (IBC).* International Code Council.

Durmaz, M., & Daloğlu, A. (2014). Türkiye Kar Verilerinin İstatistiksel Analiziyle Türk Standartlarındaki Zemin Kar Yüklerinin Değerlendirilmesi. *İMO Teknik Dergi*, 6889-6908.

Ellingwood, B., & Redfield, R. (1983). Ground Snow Loads For Structural Design. *Journal of Structural Engineering*, 950-964.

Engineering Risk and Claims Assessment for Claims Service and Underwriters. (2018). *Risk and Engineering Group Bulletin (Ekol Loss Adjusting)*, 1-34.

Eurocode 1 - Actions on structures - Part 1-3: General actions-Snow Loads. (2003). Brussels: European Committee for Standardization (CEN).

Goodison, B. E., Louie, P., & Yang, D. (1998). *WMO Solid Precipitation Measurement Intercomparison-Final Report.* World Meteorological Organization.

Grammou, N., Pertermann, I., & Puthli, R. (2019). Snow Loads on Flat Roofs with Elevated Solar Panel Arrays-Research results for wind-induced shape coefficients. *Steel Construction, 12*(4), 364-371.

International Code Council. (2012). *2012 International Building Code.* Illinois, USA: International Code Council.

International Code Council. (2015). *2015 International Building Code.* Illinois, USA: International Code Council.

Izumi, M., Nakamura, T., & Sacks, R. R. (1997). *Snow Engineering-Recent Advances.*

Kereush, D., & Perovych, I. (2017). Determinin Criteria For Optimal Site Selection For Solar Power Plants. *Geomatics, Landmanagement and Landscape*, 39-54.

Kereush, D., & Perovych, I. (2017). Determining Criteria for Optimal Site Selection for Solar Power Plants. *Geomatics, Landmanagement and Landscape*, 39-54.

Nazlıer, M., Bağzık, İ., & Eroğlu, E. (2017). Engineering Risk and Claims Assessment for Claims Service and Underwriters. *Risk and Engineering Group Bulletin (Ekol Loss Adjusting)*, 1-30.

O'Rourke, M., & Isyumov, N. (2016). *Snow Loads on Solar-Paneled Roofs.* Reston, Virginia: American Society of Civil Engineers.

Optimal site selection for solar power plants using multi-criteria evaluation: A case study from the Ayranci region in Karaman, Turkey. (2017). *Clean Technologies and Environmental Policy, 19*, 2231-2244.

Özgen, P. (2007, September). *Türkiye'deki Çatıların Optimum Kar Yüklerinin Belirlenmesi (Unpublished Master's Thesis).* Trabzon: Karadeniz Technical University.

Rasmussen, R., BakeR, B., Kochendorfer, J., Meyers, T., Landolt, S., Fischer, A. P., . . . Gutmann, E. (2012). How Well Are We Measuring Snow:The NOAA/FAA/NCAR Winter Precipitation Test Bed. *Bulletin of the American Meteorological Society*, 811-830.

Rózsás, A., & Sýkora, M. (2016). Propagating Snow Measurement Uncertainty to Structural Reliability by Statistical and Interval-based Approaches. *7th International Workshop on Reliable Engineering Computing (REC)*, (pp. 91-110). Bochum, Germany.

Sanpaolesi, L. (1996). *Scientific Support Activity in The Field of Structural Stability of Civil Engineering Works-Snow Loads.* University of Pisa, Department of Structural Engineering.

Sanpaolesi, L. (1996). The background document for snow loads. *Basis of design and actions on structures: background and application of Eurocode 1 : IABSE Colloquium Delft 1996* (pp. 191-197). Zurich: International Association for Bridge and Structural Engineering (IABSE).

SEAC Snow Load Committee. (2007). *Colorado Ground Snow Loads.*

Setting Up A Solar Power Plant: Cost And Components. (2016). Retrieved from https://www.insolergy.com: https://www.insolergy.com/blog/solar-calculator/setting-solar-power-plant-cost-components/

(2013). *Snow Measurement Guidelines for National Weather Service Surface Observing Programs.* Silver Spring: U.S. Department of Commerce National Oceanic and Atmospheric Administration.

Sri Rama , P., Ekanki, S., & Wilfried, E. (2018). Efficiency of Photovoltaic Systems in Mountainous Areas. *2018 IEEE International Energy Conference*, (pp. 1-6). Limassol.

Tetzner, D., Thomas, E., & Allen, C. (2019). A Validation of ERA5 Reanalysis Data in the Southern Antarctic Peninsula—Ellsworth Land Region, and Its Implications for Ice Core Studies. *Geosciences, 9*(289).

Turkey's Energy Profile and Strategy. (2019). Retrieved from Republic of Turkey Ministry of Foreign Affairs: http://www.mfa.gov.tr/turkeys-energy-strategy.en.mfa

Turkish Standards Institution. (1997). Design Loads for Buildings. Ankara: Turkish Standards Institution.

Turkish Standards Institution. (2007). *Eurocode 1 – Actions on structures – Part 1-3: General actions – Snow loads.* Ankara: Turkish Standards Institution.

APPENDICES

A. COMPARISON TABLES

Table A. 1- Comparison of SWE Annual Maxima Time Series of ERA5 and TSMS Stations

Station No	City	Station Name	n	NBIAS	NMAE	NRMSE	R	p value
9015	Ankara	ANKARA-TOPRAKSU	16	0.070	0.255	0.322	0.222	0.408
9019	Muş	ALPARSLAN	17	0.937	0.937	1.009	0.200	0.442
9028	Konya	KONYA TOPSU	14	0.272	0.320	0.547	-0.096	0.744
17022	Zonguldak	ZONGULDAK	28	0.081	0.171	0.210	0.740	0.000
17026	Sinop	SİNOP	18	0.196	0.231	0.296	0.627	0.005
17030	Samsun	SAMSUN BÖLGE	16	0.297	0.329	0.411	0.641	0.007
17033	Ordu	ORDU	25	0.204	0.300	0.379	0.337	0.099
17034	Giresun	GİRESUN	32	1.508	1.508	1.567	0.077	0.677
17037	Trabzon	TRABZON BÖLGE	19	0.424	0.524	0.647	0.144	0.557
17040	Rize	RİZE	21	0.516	0.561	0.676	0.222	0.334
17042	Artvin	HOPA	26	1.000	1.000	1.068	0.099	0.631
17045	Artvin	ARTVİN	34	0.712	0.712	0.814	0.474	0.005
17046	Ardahan	ARDAHAN	39	1.177	1.180	1.397	0.211	0.197
17050	Edirne	EDİRNE	28	0.002	0.119	0.148	0.895	0.000
17054	Tekirdağ	ÇORLU	25	0.300	0.391	0.536	0.478	0.016
17062	İstanbul	KADIKÖY RIHTIM	13	-0.196	0.207	0.266	0.605	0.028
17069	Sakarya	SAKARYA	28	0.184	0.234	0.288	0.557	0.002
17070	Bolu	BOLU	33	0.220	0.234	0.377	0.423	0.014
17074	Kastamonu	KASTAMONU	35	0.518	0.529	0.695	0.452	0.006
17080	Çankırı	ÇANKIRI	25	0.030	0.152	0.213	0.626	0.001
17084	Çorum	ÇORUM	29	0.066	0.092	0.111	0.915	0.000
17085	Amasya	AMASYA	22	0.293	0.331	0.442	0.557	0.007
17086	Tokat	TOKAT	28	0.528	0.528	0.639	0.361	0.059
17088	Gümüşhane	GÜMÜŞHANE	34	0.984	0.984	1.040	0.381	0.026
17089	Bayburt	BAYBURT	39	0.541	0.544	0.631	0.314	0.051
17090	Sivas	SİVAS	37	0.033	0.092	0.124	0.888	0.000
17094	Erzincan	ERZİNCAN	29	2.274	2.274	2.373	0.164	0.394
17096	Erzurum	ERZURUM HAVALİMANI	28	0.826	0.826	0.958	0.178	0.364
17097	Kars	KARS	39	0.733	0.745	0.882	0.223	0.173
17099	Ağrı	AĞRI	35	-0.062	0.112	0.190	0.593	0.000

17100	Iğdır	IĞDIR	14	0.275	0.285	0.316	0.829	0.000
17116	Bursa	BURSA	21	0.213	0.222	0.290	0.878	0.000
17120	Bilecik	BİLECİK	29	-0.087	0.120	0.182	0.679	0.000
17130	Ankara	ANKARA BÖLGE	27	0.112	0.192	0.270	0.527	0.005
17140	Yozgat	YOZGAT	37	-0.090	0.132	0.203	0.534	0.001
17155	Kütahya	KÜTAHYA	35	0.104	0.118	0.139	0.909	0.000
17160	Kırşehir	KIRŞEHİR	25	0.134	0.150	0.184	0.843	0.000
17162	Sivas	GEMEREK	31	0.494	0.496	0.595	0.752	0.000
17165	Tunceli	TUNCELİ	35	0.117	0.235	0.267	0.338	0.047
17172	Van	VAN BÖLGE	38	0.219	0.244	0.316	0.461	0.004
17188	Uşak	UŞAK	24	0.304	0.330	0.373	0.854	0.000
17190	Afyonkarahisar	AFYONKARAHİSAR BÖLGE	35	0.139	0.164	0.220	0.827	0.000
17192	Aksaray	AKSARAY	32	0.107	0.178	0.217	0.527	0.002
17193	Nevşehir	NEVŞEHİR	39	-0.061	0.127	0.194	0.545	0.000
17196	Kayseri	KAYSERİ BÖLGE	33	0.361	0.375	0.475	0.513	0.002
17199	Malatya	MALATYA	24	1.273	1.273	1.353	0.352	0.091
17201	Elazığ	ELAZIĞ BÖLGE	31	0.277	0.284	0.406	0.453	0.011
17203	Bingöl	BİNGÖL	37	0.282	0.319	0.369	0.404	0.013
17205	Bitlis	TATVAN	38	0.103	0.176	0.234	0.351	0.031
17210	Siirt	SİİRT	27	0.542	0.542	0.765	0.694	0.000
17238	Burdur	BURDUR	14	-0.001	0.179	0.219	0.454	0.103
17239	Konya	AKŞEHİR	35	-0.006	0.157	0.202	0.488	0.003
17240	Isparta	ISPARTA	27	0.001	0.128	0.186	0.488	0.010
17244	Konya	KONYA HAVALİMANI	21	0.364	0.364	0.437	0.644	0.002
17246	Karaman	KARAMAN	27	0.015	0.177	0.239	0.676	0.000
17250	Niğde	NİĞDE	35	1.137	1.140	1.384	0.253	0.142
17255	Kahramanmaraş	KAHRAMANMARAŞ	13	0.203	0.335	0.374	0.083	0.789
17265	Adıyaman	ADIYAMAN	13	0.053	0.135	0.186	0.786	0.001
17280	Diyarbakır	DİYARBAKIR HAVALİMANI	19	0.209	0.245	0.336	0.491	0.033
17285	Hakkari	HAKKARİ	39	0.527	0.538	0.583	0.010	0.951
17606	Kastamonu	KASTAMONU/BOZKURT	25	0.128	0.192	0.269	0.257	0.215
17628	Rize	RİZE/PAZAR	10	1.042	1.042	1.073	0.504	0.137
17632	Edirne	İPSALA	14	-0.144	0.156	0.245	0.797	0.001
17666	Erzurum	İSPİR	14	2.617	2.617	2.729	0.117	0.689
17680	Ankara	BEYPAZARI	22	0.081	0.162	0.240	0.208	0.354
17690	Erzurum	HORASAN	25	0.293	0.312	0.389	0.729	0.000
17692	Kars	SARIKAMIŞ	32	0.056	0.171	0.211	0.630	0.000
17700	Balıkesir	DURSUNBEY	21	0.057	0.147	0.171	0.713	0.000
17716	Sivas	ZARA	26	0.920	0.920	1.018	0.385	0.052

17718	Erzincan	TERCAN	24	0.939	0.939	1.025	0.457	0.025
17720	Ağrı	DOĞUBEYAZIT	26	0.214	0.254	0.307	0.381	0.055
17726	Eskişehir	SIVRIHISAR	29	-0.048	0.144	0.178	0.720	0.000
17728	Ankara	POLATLI	11	-0.003	0.242	0.331	0.324	0.331
17734	Sivas	DİVRİĞİ	26	1.346	1.346	1.484	0.024	0.908
17740	Erzurum	HINIS	26	-0.031	0.174	0.226	0.769	0.000
17750	Kütahya	GEDİZ	16	0.662	0.662	0.793	0.133	0.624
17752	Afyonkarahisar	EMİRDAĞ	23	0.090	0.149	0.184	0.777	0.000
17760	Yozgat	BOĞAZLIYAN	20	0.197	0.232	0.270	0.630	0.003
17762	Sivas	KANGAL	18	0.345	0.356	0.496	0.375	0.125
17764	Malatya	ARAPGİR	28	-0.142	0.178	0.235	0.647	0.000
17776	Bingöl	SOLHAN	26	0.571	0.571	0.621	0.579	0.002
17784	Van	ERCİŞ	30	-0.031	0.160	0.227	0.497	0.005
17786	Van	MURADIYE VAN	11	0.116	0.280	0.378	-0.012	0.971
17786	Van	MURADIYE VAN	11	0.116	0.280	0.378	-0.012	0.971
17802	Kayseri	KAYSERİ/PINARBAŞI	21	0.622	0.622	0.731	0.453	0.039
17804	Elazığ	KEBAN	12	0.502	0.556	0.612	0.342	0.276
17810	Bitlis	AHLAT	22	-0.102	0.108	0.205	0.530	0.011
17812	Van	ÖZALP	27	0.064	0.199	0.266	0.377	0.052
17826	Isparta	SENİRKENT	12	0.100	0.204	0.235	0.674	0.016
17837	Kayseri	TOMARZA	25	0.280	0.336	0.510	0.282	0.172
17847	Diyarbakır	ERGANİ	23	0.033	0.121	0.153	0.824	0.000
17866	Kahramanmaraş	GÖKSUN	31	0.433	0.438	0.499	0.498	0.004
17870	Kahramanmaraş	ELBİSTAN	27	0.985	0.985	1.206	0.167	0.405
17880	Van	BAŞKALE	33	0.065	0.130	0.163	0.658	0.000
17882	Isparta	EĞİRDİR	17	-0.089	0.186	0.243	0.594	0.012
17906	Niğde	ULUKIŞLA	32	1.215	1.216	1.431	0.237	0.192
17920	Hakkari	YÜKSEKOVA	29	0.262	0.285	0.323	0.403	0.030
17928	Konya	HADİM	28	0.583	0.588	0.703	0.660	0.000
17952	Antalya	ELMALI	15	1.912	1.912	2.212	0.331	0.229

Table A. 2- Comparison of Snow Depth Annual Maxima Time Series of ERA5 and TSMS Stations

Station No	City	Station Name	n	NBIAS	NMAE	NRMSE	R	p value
3012	Bolu	SERIFYUK-ALADAG	15	-0.433	0.433	0.447	0.754	0.001
3018	Tokat	TOKAT TOP.SU	19	0.464	0.464	0.537	0.603	0.006
9013	Zonguldak	BAKLABOSTAN	10	-0.279	0.279	0.354	0.648	0.043
9014	Ankara	BALA DUC	14	-0.019	0.167	0.206	0.610	0.021
9015	Ankara	ANKARA-TOPRAKSU	22	-0.060	0.199	0.249	0.660	0.001
9016	Ankara	CAMKORU	18	-0.181	0.203	0.261	0.708	0.001
9017	Bolu	BAKACAK	22	-0.387	0.387	0.427	0.449	0.036
9019	Muş	ALPARSLAN	19	0.348	0.349	0.405	0.577	0.010
9023	Konya	GOZLU DUC	18	-0.057	0.134	0.168	0.740	0.000
9025	Konya	ALTINOVA DUC	16	-0.084	0.145	0.211	0.554	0.026
9027	Eskişehir	ESKISEHIR TOPSU	16	0.164	0.181	0.260	0.707	0.002
9028	Konya	KONYA TOPSU	19	0.037	0.146	0.228	0.464	0.045
9035	Konya	KONUKLAR	13	-0.005	0.146	0.207	0.565	0.044
17015	Düzce	AKÇAKOCA	33	0.088	0.214	0.265	0.274	0.122
17020	Bartın	BARTIN	38	-0.063	0.136	0.173	0.843	0.000
17022	Zonguldak	ZONGULDAK	39	0.010	0.105	0.136	0.831	0.000
17024	Kastamonu	İNEBOLU	38	0.165	0.212	0.261	0.355	0.029
17026	Sinop	SİNOP	31	0.015	0.138	0.175	0.626	0.000
17030	Samsun	SAMSUN BÖLGE	35	0.091	0.234	0.280	0.535	0.001
17031	Samsun	SAMSUN ÇARŞAMBA HAVALİMANI	18	-0.054	0.103	0.202	0.724	0.001
17033	Ordu	ORDU	36	0.034	0.206	0.260	0.328	0.051
17034	Giresun	GİRESUN	36	0.784	0.784	0.820	0.432	0.008
17037	Trabzon	TRABZON BÖLGE	27	0.232	0.303	0.378	0.324	0.099
17038	Trabzon	TRABZON HAVALİMANI	18	0.067	0.223	0.280	0.198	0.432
17040	Rize	RİZE	36	0.333	0.427	0.494	0.199	0.246
17042	Artvin	HOPA	37	0.748	0.748	0.790	0.208	0.217
17045	Artvin	ARTVİN	39	0.418	0.423	0.485	0.477	0.002
17046	Ardahan	ARDAHAN	40	0.384	0.399	0.475	0.359	0.023
17050	Edirne	EDİRNE	39	-0.034	0.072	0.106	0.947	0.000
17052	Kırklareli	KIRKLARELİ	31	0.255	0.293	0.384	0.569	0.001
17054	Tekirdağ	ÇORLU	33	-0.110	0.194	0.274	0.529	0.002
17056	Tekirdağ	TEKİRDAĞ	38	-0.091	0.106	0.184	0.883	0.000
17059	İstanbul	SARIYER/KUMKÖY-KİLYOS	32	-0.019	0.098	0.174	0.509	0.003

17060	İstanbul	İSTANBUL ATATÜRK HAVALİMANI	15	-0.236	0.262	0.310	0.598	0.018
17061	İstanbul	SARIYER	37	-0.158	0.161	0.248	0.587	0.000
17062	İstanbul	KADIKÖY RIHTIM	29	-0.241	0.243	0.331	0.613	0.000
17066	Kocaeli	KOCAELİ	35	-0.004	0.127	0.172	0.674	0.000
17067	Kocaeli	GÖLCÜK	13	0.145	0.176	0.210	0.821	0.001
17068	Kocaeli	KOCAELİ CENGİZ TOPEL HAVALİMANI	10	-0.105	0.260	0.318	0.627	0.052
17069	Sakarya	SAKARYA	39	0.002	0.144	0.199	0.678	0.000
17070	Bolu	BOLU	40	0.003	0.132	0.196	0.543	0.000
17072	Düzce	DÜZCE	39	0.016	0.192	0.249	0.396	0.012
17074	Kastamonu	KASTAMONU	40	0.426	0.438	0.558	0.663	0.000
17078	Karabük	KARABUK	19	0.515	0.540	0.642	0.335	0.161
17080	Çankırı	ÇANKIRI	37	0.010	0.126	0.167	0.772	0.000
17083	Amasya	MERZİFON	35	0.218	0.276	0.368	0.502	0.002
17084	Çorum	ÇORUM	40	0.013	0.064	0.093	0.935	0.000
17085	Amasya	AMASYA	40	0.063	0.124	0.169	0.748	0.000
17086	Tokat	TOKAT	40	0.387	0.387	0.468	0.598	0.000
17088	Gümüşhane	GÜMÜŞHANE	40	0.823	0.823	0.861	0.639	0.000
17089	Bayburt	BAYBURT	40	0.346	0.347	0.404	0.523	0.001
17090	Sivas	SİVAS	40	0.005	0.024	0.046	0.982	0.000
17092	Erzincan	ERZİNCAN HAVALİMANI	19	0.691	0.691	0.729	0.487	0.034
17094	Erzincan	ERZİNCAN	40	0.721	0.727	0.769	0.272	0.090
17095	Erzurum	ERZURUM BÖLGE	10	0.097	0.152	0.201	0.696	0.026
17096	Erzurum	ERZURUM HAVALİMANI	40	0.272	0.272	0.319	0.606	0.000
17097	Kars	KARS	40	0.264	0.271	0.310	0.712	0.000
17098	Kars	KARS HARAKANİ HAVALİMANI	19	0.155	0.159	0.170	0.959	0.000
17099	Ağrı	AĞRI	40	-0.113	0.121	0.165	0.726	0.000
17100	Iğdır	IĞDIR	39	0.240	0.291	0.414	0.446	0.004
17110	Çanakkale	GÖKÇEADA	27	-0.235	0.241	0.313	0.729	0.000
17111	Çanakkale	BOZCAADA	10	0.233	0.263	0.335	0.626	0.053
17112	Çanakkale	ÇANAKKALE	33	0.037	0.079	0.129	0.813	0.000
17114	Balıkesir	BANDIRMA	27	0.199	0.262	0.406	0.610	0.001
17115	Balıkesir	BANDIRMA HAVALİMANI	15	-0.043	0.064	0.141	0.890	0.000
17116	Bursa	BURSA	34	-0.013	0.061	0.082	0.924	0.000
17118	Bursa	BURSA YENİŞEHİR HAVALİMANI	13	0.179	0.269	0.403	0.426	0.147
17119	Yalova	YALOVA	30	0.102	0.187	0.267	0.467	0.009
17120	Bilecik	BİLECİK	40	-0.081	0.126	0.169	0.585	0.000
17123	Eskişehir	ESKİŞEHİR HASAN P.ü HAVALİMANI	23	0.239	0.246	0.301	0.809	0.000

17124	Eskişehir	ESKİŞEHİR HAVALİMANI	21	0.078	0.083	0.102	0.972	0.000
17126	Eskişehir	ESKİŞEHİR BÖLGE	11	-0.022	0.139	0.199	0.782	0.004
17127	Ankara	ANKARA MÜRTED HAVALİMANI	11	-0.071	0.156	0.201	0.828	0.002
17128	Ankara	ANKARA ESENBOĞA HAVALİMANI	39	0.009	0.057	0.078	0.949	0.000
17129	Ankara	ETİMESGUT HAVALİMANI	22	0.114	0.140	0.201	0.854	0.000
17130	Ankara	ANKARA BÖLGE	38	-0.008	0.122	0.155	0.834	0.000
17135	Kırıkkale	KIRIKKALE	38	-0.003	0.101	0.145	0.814	0.000
17140	Yozgat	YOZGAT	40	-0.145	0.145	0.206	0.689	0.000
17150	Balıkesir	BALIKESİR HAVALİMANI	19	0.081	0.136	0.171	0.899	0.000
17155	Kütahya	KÜTAHYA	40	-0.041	0.081	0.110	0.918	0.000
17160	Kırşehir	KIRŞEHİR	39	0.055	0.107	0.123	0.868	0.000
17162	Sivas	GEMEREK	38	0.219	0.231	0.298	0.790	0.000
17165	Tunceli	TUNCELİ	40	0.114	0.198	0.229	0.560	0.000
17170	Van	VAN FERİT MELEN HAVALİMANI	19	0.081	0.135	0.164	0.842	0.000
17172	Van	VAN BÖLGE	40	0.049	0.094	0.145	0.587	0.000
17175	Balıkesir	AYVALIK	10	-0.166	0.184	0.240	0.879	0.001
17180	İzmir	DİKİLİ	10	0.392	0.487	0.683	0.370	0.293
17184	Manisa	AKHİSAR	16	0.207	0.253	0.355	0.530	0.035
17186	Manisa	MANİSA	16	-0.104	0.217	0.285	0.719	0.002
17188	Uşak	UŞAK	36	0.062	0.077	0.101	0.937	0.000
17189	Afyonkarahisar	AFYONKARAHİSAR HAVALİMANI	10	-0.031	0.122	0.208	0.811	0.004
17190	Afyonkarahisar	AFYONKARAHİSAR BÖLGE	38	-0.056	0.078	0.118	0.915	0.000
17191	Konya	CİHANBEYLİ	40	-0.209	0.221	0.287	0.662	0.000
17192	Aksaray	AKSARAY	40	-0.037	0.121	0.153	0.707	0.000
17193	Nevşehir	NEVŞEHİR	40	-0.147	0.152	0.187	0.776	0.000
17195	Kayseri	KAYSERİ ERKİLET HAVALİMANI	19	0.296	0.309	0.388	0.686	0.001
17196	Kayseri	KAYSERİ BÖLGE	40	0.160	0.192	0.270	0.672	0.000
17199	Malatya	MALATYA	40	0.794	0.794	0.874	0.292	0.068
17200	Malatya	MALATYA ERHAÇ HAVALİMANI	13	0.138	0.201	0.256	0.718	0.006
17201	Elazığ	ELAZIĞ BÖLGE	39	0.117	0.147	0.224	0.703	0.000
17202	Elazığ	ELAZIĞ HAVALİMANI	17	0.034	0.058	0.081	0.944	0.000
17203	Bingöl	BİNGÖL	40	0.206	0.227	0.269	0.532	0.000
17204	Muş	MUŞ	40	0.177	0.206	0.248	0.674	0.000
17205	Bitlis	TATVAN	38	0.053	0.142	0.194	0.612	0.000
17210	Siirt	SİİRT	36	0.237	0.248	0.385	0.607	0.000
17234	Aydın	AYDIN	10	0.018	0.286	0.366	0.593	0.071
17237	Denizli	DENİZLİ	31	-0.092	0.107	0.144	0.861	0.000

17238	Burdur	BURDUR	38	-0.005	0.109	0.170	0.561	0.000
17239	Konya	AKŞEHİR	40	-0.131	0.174	0.223	0.619	0.000
17240	Isparta	ISPARTA	40	0.084	0.163	0.246	0.647	0.000
17242	Konya	BEYŞEHİR	40	0.031	0.148	0.225	0.549	0.000
17244	Konya	KONYA HAVALİMANI	40	0.082	0.093	0.129	0.895	0.000
17246	Karaman	KARAMAN	40	-0.054	0.069	0.102	0.875	0.000
17248	Konya	EREĞLİ	40	0.025	0.087	0.134	0.816	0.000
17250	Niğde	NİĞDE	40	0.479	0.496	0.601	0.434	0.005
17255	Kahramanmaraş	KAHRAMANMARAŞ	28	0.077	0.167	0.234	0.585	0.001
17260	Gaziantep	GAZİANTEP HAVALİMANI	15	-0.074	0.074	0.131	0.940	0.000
17261	Gaziantep	GAZİANTEP	37	-0.085	0.127	0.173	0.720	0.000
17262	Kilis	KİLİS	24	0.030	0.105	0.155	0.675	0.000
17265	Adıyaman	ADIYAMAN	31	0.141	0.170	0.223	0.575	0.001
17270	Şanlıurfa	ŞANLIURFA	23	0.103	0.142	0.199	0.733	0.000
17275	Mardin	MARDİN	36	-0.104	0.125	0.176	0.565	0.000
17280	Diyarbakır	DİYARBAKIR HAVALİMANI	35	0.072	0.111	0.175	0.856	0.000
17282	Batman	BATMAN	30	0.234	0.317	0.443	0.393	0.032
17285	Hakkari	HAKKARİ	40	0.156	0.228	0.250	0.286	0.074
17292	Muğla	MUĞLA	23	0.060	0.131	0.183	0.766	0.000
17372	Hatay	ANTAKYA	13	-0.186	0.230	0.312	0.688	0.009
17602	Bartın	AMASRA	32	0.131	0.181	0.221	0.787	0.000
17604	Kastamonu	CİDE	14	0.639	0.654	0.728	0.638	0.014
17606	Kastamonu	KASTAMONU/BOZKURT	33	0.048	0.136	0.180	0.396	0.022
17608	Edirne	UZUNKÖPRÜ	32	-0.109	0.116	0.173	0.828	0.000
17610	İstanbul	ŞİLE	30	-0.083	0.161	0.231	0.432	0.017
17618	Kastamonu	DEVREKANİ	32	-0.029	0.158	0.197	0.581	0.000
17622	Samsun	BAFRA	31	-0.161	0.211	0.290	0.413	0.021
17624	Ordu	ÜNYE	33	0.359	0.463	0.547	0.313	0.077
17626	Trabzon	AKÇAABAT	30	0.426	0.494	0.591	0.379	0.039
17628	Rize	RİZE/PAZAR	32	1.027	1.027	1.066	0.394	0.025
17631	Kırklareli	LÜLEBURGAZ TİGEM	27	0.064	0.096	0.130	0.874	0.000
17632	Edirne	İPSALA	31	-0.106	0.126	0.188	0.836	0.000
17634	Tekirdağ	MALKARA	31	-0.107	0.125	0.184	0.779	0.000
17636	İstanbul	FLORYA	33	-0.157	0.179	0.241	0.511	0.002
17646	Çankırı	ÇERKEŞ	32	0.302	0.364	0.448	0.437	0.012
17648	Çankırı	ILGAZ	33	0.481	0.492	0.580	0.632	0.000
17650	Kastamonu	TOSYA	33	0.279	0.295	0.387	0.472	0.006
17652	Çorum	OSMANCIK	12	0.228	0.228	0.248	0.938	0.000
17656	Kars	ARPAÇAY	32	0.179	0.238	0.301	0.446	0.010

17658	Yalova	ÇINARCIK	21	0.224	0.351	0.472	0.429	0.052
17662	Sakarya	GEYVE	32	0.040	0.205	0.261	0.351	0.049
17664	Ankara	KIZILCAHAMAM	34	0.170	0.199	0.286	0.514	0.002
17666	Erzurum	İSPİR	35	0.947	0.947	0.969	0.632	0.000
17668	Erzurum	OLTU	35	0.750	0.750	0.809	0.552	0.001
17674	Balıkesir	BALIKESİR/GÖNEN	30	0.059	0.204	0.293	0.567	0.001
17676	Bursa	ULUDAĞ	39	-0.513	0.515	0.558	0.240	0.141
17678	Bursa	YENISEHIR	18	-0.010	0.124	0.157	0.857	0.000
17679	Ankara	NALLIHAN	12	0.183	0.296	0.374	0.176	0.585
17680	Ankara	BEYPAZARI	34	0.071	0.137	0.191	0.394	0.021
17681	Tokat	ZİLE	35	0.023	0.127	0.164	0.660	0.000
17682	Giresun	ŞEBİNKARAHİSAR	35	0.506	0.506	0.553	0.687	0.000
17683	Tokat	TURHAL	15	0.045	0.147	0.205	0.674	0.006
17684	Sivas	SUŞEHRİ	32	0.476	0.476	0.517	0.625	0.000
17688	Erzurum	TORTUM	35	0.491	0.491	0.542	0.557	0.001
17690	Erzurum	HORASAN	35	0.160	0.207	0.266	0.432	0.010
17692	Kars	SARIKAMIŞ	35	0.009	0.142	0.179	0.607	0.000
17695	Bursa	KELES	34	0.021	0.154	0.197	0.543	0.001
17700	Balıkesir	DURSUNBEY	34	0.013	0.144	0.186	0.581	0.000
17702	Bilecik	BOZÜYÜK	34	-0.179	0.209	0.261	0.603	0.000
17704	Kütahya	TAVŞANLI	34	0.026	0.211	0.264	0.475	0.005
17712	Yozgat	SORGUN	19	0.190	0.202	0.246	0.840	0.000
17716	Sivas	ZARA	35	0.689	0.689	0.736	0.649	0.000
17718	Erzincan	TERCAN	35	0.552	0.552	0.611	0.567	0.000
17720	Ağrı	DOĞUBEYAZIT	33	0.345	0.350	0.429	0.637	0.000
17726	Eskişehir	SIVRIHISAR	34	-0.099	0.158	0.202	0.638	0.000
17728	Ankara	POLATLI	34	-0.052	0.132	0.171	0.646	0.000
17730	Kırıkkale	KESKİN	32	-0.102	0.167	0.209	0.674	0.000
17732	Kırşehir	ÇİÇEKDAĞI	33	-0.018	0.145	0.181	0.630	0.000
17734	Sivas	DİVRİĞİ	35	0.985	0.985	1.068	0.397	0.018
17736	Tunceli	MAZGİRT	33	-0.055	0.132	0.184	0.638	0.000
17740	Erzurum	HINIS	35	0.008	0.150	0.188	0.611	0.000
17746	Manisa	DEMİRCİ	21	-0.014	0.226	0.316	0.252	0.270
17748	Kütahya	SİMAV	34	-0.134	0.192	0.255	0.516	0.002
17750	Kütahya	GEDİZ	31	0.301	0.311	0.386	0.542	0.002
17752	Afyonkarahisar	EMİRDAĞ	33	0.019	0.110	0.138	0.855	0.000
17754	Konya	KULU	35	-0.121	0.126	0.185	0.818	0.000
17756	Kırşehir	KAMAN	34	-0.261	0.273	0.333	0.566	0.000
17760	Yozgat	BOĞAZLIYAN	35	0.122	0.179	0.227	0.747	0.000
17762	Sivas	KANGAL	35	0.005	0.187	0.245	0.345	0.043

17764	Malatya	ARAPGİR	34	-0.143	0.208	0.251	0.604	0.000
17766	Elazığ	AĞIN	33	0.484	0.498	0.566	0.378	0.030
17768	Tunceli	ÇEMİŞGEZEK	34	0.561	0.561	0.632	0.390	0.023
17774	Elazığ	KARAKOÇAN	33	1.167	1.174	1.320	0.287	0.105
17776	Bingöl	SOLHAN	35	0.503	0.503	0.549	0.609	0.000
17778	Muş	VARTO	29	0.318	0.328	0.396	0.535	0.003
17780	Muş	MALAZGİRT	35	-0.160	0.186	0.227	0.755	0.000
17784	Van	ERCİŞ	35	0.014	0.132	0.164	0.548	0.001
17786	Van	MURADIYE VAN	35	-0.034	0.125	0.157	0.706	0.000
17786	Van	MURADIYE VAN	35	-0.034	0.125	0.157	0.706	0.000
17792	Manisa	SALİHLİ	16	0.003	0.145	0.202	0.768	0.001
17793	Afyonkarahisar	ÇAY	11	-0.136	0.219	0.282	0.459	0.155
17796	Afyonkarahisar	BOLVADİN	33	0.033	0.119	0.171	0.741	0.000
17798	Konya	YUNAK	29	-0.165	0.195	0.247	0.392	0.035
17802	Kayseri	KAYSERİ/PINARBAŞI	33	0.347	0.351	0.409	0.613	0.000
17804	Elazığ	KEBAN	33	0.294	0.333	0.432	0.449	0.009
17806	Elazığ	PALU	34	0.671	0.671	0.836	0.442	0.009
17808	Bingöl	GENÇ	35	0.297	0.305	0.378	0.537	0.001
17810	Bitlis	AHLAT	35	-0.075	0.114	0.170	0.524	0.001
17812	Van	ÖZALP	35	0.037	0.121	0.165	0.518	0.001
17824	Denizli	GÜNEY	27	-0.060	0.184	0.232	0.621	0.001
17826	Isparta	SENİRKENT	31	-0.007	0.127	0.164	0.669	0.000
17828	Isparta	YALVAÇ	29	0.066	0.186	0.248	0.404	0.030
17832	Konya	ILGIN	35	0.031	0.135	0.187	0.524	0.001
17833	Nevşehir	AVANOS	17	0.155	0.218	0.255	0.741	0.001
17835	Nevşehir	ÜRGÜP	35	-0.052	0.128	0.165	0.680	0.000
17836	Kayseri	DEVELİ	35	0.389	0.425	0.517	0.483	0.003
17837	Kayseri	TOMARZA	33	0.128	0.206	0.293	0.449	0.009
17840	Kayseri	SARIZ	34	0.290	0.298	0.344	0.671	0.000
17842	Malatya	DARANDE/BALABAN	24	0.366	0.428	0.561	0.279	0.187
17843	Elazığ	BASKİL	26	0.168	0.248	0.353	0.379	0.056
17844	Elazığ	SİVRİCE	35	-0.040	0.158	0.235	0.451	0.007
17846	Elazığ	MADEN	34	-0.023	0.127	0.181	0.494	0.003
17847	Diyarbakır	ERGANİ	34	0.137	0.198	0.263	0.537	0.001
17852	Van	GEVAŞ	32	0.220	0.286	0.346	0.322	0.073
17862	Afyonkarahisar	DİNAR	33	0.111	0.204	0.255	0.458	0.007
17864	Isparta	ULUBORLU	23	0.079	0.248	0.327	0.358	0.094
17866	Kahramanmaraş	GÖKSUN	36	0.432	0.443	0.495	0.596	0.000
17868	Kahramanmaraş	AFŞİN	28	0.120	0.193	0.267	0.635	0.000
17870	Kahramanmaraş	ELBİSTAN	35	0.418	0.456	0.572	0.170	0.330

17871	Adıyaman	GÖLBAŞI	15	0.072	0.143	0.168	0.905	0.000
17872	Malatya	DOĞANŞEHİR	21	0.664	0.664	0.766	0.242	0.290
17874	Diyarbakır	ÇERMİK	31	0.402	0.457	0.564	0.352	0.052
17880	Van	BAŞKALE	35	0.079	0.144	0.184	0.656	0.000
17882	Isparta	EĞİRDİR	27	0.100	0.187	0.226	0.680	0.000
17890	Denizli	ACIPAYAM	33	-0.009	0.100	0.121	0.861	0.000
17892	Burdur	TEFENNİ	33	0.043	0.171	0.230	0.322	0.068
17898	Konya	SEYDİŞEHİR	35	-0.076	0.206	0.281	0.348	0.041
17900	Konya	ÇUMRA	34	-0.030	0.136	0.179	0.613	0.000
17902	Konya	KARAPINAR	35	-0.051	0.122	0.158	0.770	0.000
17906	Niğde	ULUKIŞLA	35	0.570	0.590	0.672	0.275	0.109
17910	Adıyaman	KAHTA	14	0.158	0.172	0.217	0.819	0.000
17912	Şanlıurfa	SİVEREK	31	0.167	0.204	0.260	0.799	0.000
17914	Şanlıurfa	HİLVAN	11	-0.077	0.125	0.222	0.719	0.013
17920	Hakkari	YÜKSEKOVA	36	0.101	0.155	0.184	0.500	0.002
17926	Antalya	KORKUTELİ	32	0.141	0.188	0.257	0.428	0.015
17928	Konya	HADİM	35	0.168	0.183	0.225	0.689	0.000
17934	Adana	POZANTI	10	1.437	1.437	1.556	0.655	0.040
17952	Antalya	ELMALI	33	1.314	1.314	1.497	0.462	0.007
17964	Gaziantep	ISLAHIYE	19	0.004	0.170	0.209	0.489	0.033
17966	Şanlıurfa	BİRECİK	14	0.146	0.258	0.368	0.509	0.063

Table A. 3- Comparison of Ground Snow Loads

			kN/m^2				Error %	
Station No	**City**	**Station Name**	**SL_{st}**	**SL_G**	**a_{Int}**	**SL_{Int}**	**SL_G**	**SL_{Int}**
9019	Muş	ALPARSLAN	2,88	3,84	1,64	3,48	33%	21%
17022	Zonguldak	ZONGULDAK	1,31	1,18	0,97	0,99	-10%	-24%
17033	Ordu	ORDU	0,95	0,73	0,97	0,97	-23%	2%
17034	Giresun	GİRESUN	1,03	2,39	1,38	1,38	131%	33%
17045	Artvin	ARTVİN	3,32	4,56	2,38	3,01	37%	-9%
17046	Ardahan	ARDAHAN	1,32	3,19	0,87	2,93	142%	122%
17050	Edirne	EDİRNE	0,92	0,61	0,61	0,61	-34%	-34%
17054	Tekirdağ	ÇORLU	0,36	0,53	0,51	0,52	49%	46%
17069	Sakarya	SAKARYA	0,68	0,77	0,70	0,70	13%	2%
17070	Bolu	BOLU	1,00	1,37	0,81	1,13	37%	13%
17074	Kastamonu	KASTAMONU	0,76	1,83	1,12	1,64	141%	115%
17080	Çankırı	ÇANKIRI	0,99	0,66	0,51	0,71	-33%	-28%
17084	Çorum	ÇORUM	0,70	0,66	0,40	0,57	-6%	-19%
17086	Tokat	TOKAT	0,86	1,54	0,76	0,97	80%	13%
17088	Gümüşhane	GÜMÜŞHANE	1,47	3,63	1,39	2,86	148%	95%
17089	Bayburt	BAYBURT	1,70	2,95	0,91	2,53	74%	49%
17090	Sivas	SİVAS	1,62	1,34	0,60	1,32	-17%	-18%
17096	Erzurum	ERZURUM HAVALİMANI	1,62	3,16	0,90	2,88	95%	78%
17097	Kars	KARS	1,62	2,51	0,63	2,05	55%	27%
17099	Ağrı	AĞRI	4,86	2,09	0,67	1,95	-57%	-60%
17116	Bursa	BURSA	0,73	0,92	0,90	0,91	26%	24%
17130	Ankara	ANKARA BÖLGE	0,43	0,50	0,33	0,52	17%	20%
17140	Yozgat	YOZGAT	1,69	0,95	0,46	1,01	-44%	-40%
17155	Kütahya	KÜTAHYA	0,77	0,92	0,48	0,80	20%	3%
17160	Kırşehir	KIRŞEHİR	0,89	0,59	0,29	0,50	-33%	-44%
17162	Sivas	GEMEREK	0,98	1,40	0,65	1,30	43%	33%
17165	Tunceli	TUNCELİ	2,98	1,59	1,21	2,03	-47%	-32%
17172	Van	VAN BÖLGE	1,87	1,35	0,44	1,31	-28%	-30%
17190	Afyonkarahisar	AFYONKARAHİSAR BÖLGE	0,76	0,94	0,43	0,75	25%	-1%
17192	Aksaray	AKSARAY	0,59	0,52	0,29	0,49	-12%	-17%
17193	Nevşehir	NEVŞEHİR	1,16	0,73	0,34	0,71	-37%	-39%

17196	Kayseri	KAYSERİ BÖLGE	0,64	1,36	0,67	1,24	112%	93%
17201	Elazığ	ELAZIĞ BÖLGE	0,66	0,90	0,68	1,15	37%	75%
17203	Bingöl	BİNGÖL	4,30	4,30	1,68	3,22	0%	-25%
17205	Bitlis	TATVAN	4,37	3,13	0,89	2,63	-28%	-40%
17239	Konya	AKŞEHİR	0,88	0,96	0,45	0,76	10%	-13%
17240	Isparta	ISPARTA	1,01	0,71	0,32	0,54	-30%	-46%
17244	Konya	KONYA HAVALİMANI	0,65	0,98	0,52	0,90	50%	39%
17285	Hakkari	HAKKARİ	5,24	5,03	1,33	4,15	-4%	-21%
17606	Kastamonu	KASTAMONU/BOZKURT	2,64	3,20	1,26	1,28	21%	-52%
17692	Kars	SARIKAMIŞ	2,85	2,90	0,64	2,66	2%	-7%
17726	Eskişehir	SIVRIHISAR	0,59	0,55	0,30	0,54	-6%	-8%
17784	Van	ERCİŞ	2,41	0,94	0,42	1,26	-61%	-48%
17866	Kahramanmaraş	GÖKSUN	2,94	3,90	1,68	3,84	33%	31%
17880	Van	BAŞKALE	3,89	2,57	0,58	2,74	-34%	-30%

where;

SL_{st} : Snow load at station location

SL_G : Snow load at nearest grid point

a_{Int} : Interpolated parameter ‘a’

SL_{Int} : Interpolated snow load to station location

Table A. 4- Comparison of Proposed Map with TS498

Station No	Station Name	Ground Snow Load (kN/m2)			Percent Error (%)		Weighted Error	
		Station	Proposed Map	TS498	Proposed	TS498	Proposed	TS498
17192	AKSARAY	0,59	0,49	0,8	-17%	35%	-0,10	0,21
17160	KIRŞEHİR	0,89	0,5	0,88	-44%	-1%	-0,39	-0,01
17130	ANKARA BÖLGE	0,43	0,52	1,16	20%	168%	0,09	0,72
17054	ÇORLU	0,36	0,52	0,75	46%	109%	0,17	0,39
17726	SIVRIHISAR	0,59	0,54	1,16	-8%	96%	-0,05	0,57
17240	ISPARTA	1,01	0,54	1,05	-46%	4%	-0,46	0,04
17084	ÇORUM	0,7	0,57	0,95	-19%	36%	-0,13	0,25
17050	EDİRNE	0,92	0,61	0,75	-34%	-18%	-0,31	-0,17
17069	SAKARYA	0,68	0,7	0,75	2%	10%	0,01	0,07
17080	ÇANKIRI	0,99	0,71	1,25	-28%	26%	-0,28	0,26
17193	NEVŞEHİR	1,16	0,71	0,88	-39%	-24%	-0,45	-0,28
17190	AFYONKARAHİSAR BÖLGE	0,76	0,75	1,49	-1%	97%	-0,01	0,74
17239	AKŞEHİR	0,88	0,76	1,05	-13%	20%	-0,11	0,18
17155	KÜTAHYA	0,77	0,8	1,35	3%	75%	0,02	0,58
17244	KONYA HAVALİMANI	0,65	0,9	1,05	39%	61%	0,25	0,40
17116	BURSA	0,73	0,91	0,75	24%	2%	0,18	0,01
17086	TOKAT	0,86	0,97	0,85	13%	-1%	0,11	-0,01
17033	ORDU	0,95	0,97	0,75	2%	-21%	0,02	-0,20
17022	ZONGULDAK	1,31	0,99	0,75	-24%	-43%	-0,31	-0,56
17140	YOZGAT	1,69	1,01	1,49	-40%	-12%	-0,68	-0,20
17070	BOLU	1	1,13	1,25	13%	25%	0,13	0,25
17201	ELAZIĞ BÖLGE	0,66	1,15	1,35	75%	105%	0,50	0,69
17196	KAYSERİ BÖLGE	0,64	1,24	0,88	93%	37%	0,60	0,24
17784	ERCİŞ	2,41	1,26	1,84	-48%	-24%	-1,16	-0,58
17606	KASTAMONU/BOZKURT	2,64	1,28	0,75	-52%	-72%	-1,37	-1,90
17162	GEMEREK	0,98	1,3	1,49	33%	52%	0,32	0,51
17172	VAN BÖLGE	1,87	1,31	1,84	-30%	-2%	-0,56	-0,04
17090	SİVAS	1,62	1,32	1,49	-18%	-8%	-0,29	-0,13
17034	GİRESUN	1,03	1,38	0,75	33%	-27%	0,34	-0,28
17074	KASTAMONU	0,76	1,64	1,25	115%	65%	0,87	0,49
17099	AĞRI	4,86	1,95	1,84	-60%	-62%	-2,92	-3,01
17165	TUNCELİ	2,98	2,03	1,6	-32%	-46%	-0,95	-1,37
17097	KARS	1,62	2,05	1,84	27%	13%	0,44	0,21
17089	BAYBURT	1,7	2,53	1,55	49%	-8%	0,83	-0,14

17205	TATVAN	4,37	2,63	1,84	-40%	-58%	-1,75	-2,53
17692	SARIKAMIŞ	2,85	2,66	1,84	-7%	-35%	-0,20	-1,00
17880	BAŞKALE	3,89	2,74	1,84	-30%	-53%	-1,17	-2,06
17088	GÜMÜŞHANE	1,47	2,86	1,49	95%	1%	1,40	0,01
17096	ERZURUM HAVALİMANI	1,62	2,88	1,55	78%	-4%	1,26	-0,06
17046	ARDAHAN	1,32	2,93	1,84	122%	39%	1,61	0,51
17045	ARTVİN	3,32	3,01	0,95	-9%	-71%	-0,30	-2,36
17203	BİNGÖL	4,3	3,22	1,76	-25%	-59%	-1,08	-2,54
9019	ALPARSLAN	2,88	3,48	1,76	21%	-39%	0,60	-1,12
17866	GÖKSUN	2,94	3,84	1,49	31%	-49%	0,91	-1,44
17285	HAKKARİ	5,24	4,15	1,84	-21%	-65%	-1,10	-3,41
	Average	1,69	1,57	1,29	6%	6%	-0,12	-0,40
	Weighted Avg. Error %						-7,21%	-23,80%

Table A. 5- Comparison of Proposed Snow Load Values with TS498

No	İl	Latitude	Longitude	Altitude (m)	Proposed Snow Load (kN/m2)	Region	TS498 Snow Load (kN/m2)	Diff. %
1	ADANA	37	35,321333	17	0,10	I	0,75	86%
2	ADIYAMAN	37,764751	38,278561	676	0,93	II	0,75	-24%
3	AFYONKARAHİSAR	38,750714	30,556692	1011	0,74	III	1,485	50%
4	AĞRI	39,626922	43,021596	1658	1,76	IV	1,84	4%
5	AKSARAY	38,36869	34,03698	971	0,50	I	0,8	38%
6	AMASYA	40,64991	35,83532	455	0,58	III	0,75	22%
7	ANKARA	39,92077	32,85411	855	0,50	II	0,95	48%
8	ANTALYA	36,88414	30,70563	26	0,27	I	0,75	63%
9	ARDAHAN	41,110481	42,702171	1809	2,92	IV	1,84	-59%
10	ARTVİN	41,18277	41,818292	615	3,00	IV	0,95	-216%
11	AYDIN	37,856041	27,841631	158	0,18	I	0,75	77%
12	BALIKESİR	39,648369	27,88261	153	0,66	I	0,75	13%
13	BARTIN	41,581051	32,460979	496	1,27	III	0,75	-69%
14	BATMAN	37,881168	41,13509	572	0,64	II	0,75	15%
15	BAYBURT	40,255169	40,22488	1557	2,49	III	1,5525	-60%
16	BİLECİK	40,056656	30,066524	615	0,73	III	0,85	14%
17	BİNGÖL	39,062635	40,76961	1446	3,18	IV	1,76	-80%
18	BİTLİS	38,393799	42,12318	1495	2,66	IV	1,76	-51%
19	BOLU	40,575977	31,578809	1469	1,73	III	1,485	-17%
20	BURDUR	37,461267	30,066524	1006	0,35	II	1,155	69%
21	BURSA	40,266864	29,063448	84	0,85	IV	0,75	-13%
22	ÇANAKKALE	40,155312	26,41416	11	0,65	I	0,75	14%
23	ÇANKIRI	40,601343	33,613421	741	0,69	III	1,25	45%
24	ÇORUM	40,550556	34,955556	819	0,59	II	0,95	37%
25	DENİZLİ	37,77652	29,08639	397	0,32	II	0,75	57%
26	DİYARBAKIR	37,91441	40,230629	667	0,60	II	0,75	20%
27	DÜZCE	40,843849	31,15654	156	0,81	III	0,75	-8%
28	EDİRNE	41,681808	26,562269	55	0,61	III	0,75	19%
29	ELAZIĞ	38,680969	39,226398	1096	1,07	III	1,485	28%
30	ERZİNCAN	39,75	39,5	1200	3,78	III	1,485	-154%
31	ERZURUM	39,9	41,27	1938	3,12	III	1,5525	-101%
32	ESKİŞEHİR	39,776667	30,520556	805	0,74	II	0,95	22%
33	GAZİANTEP	37,06622	37,38332	861	0,49	III	1,3	62%
34	GİRESUN	40,912811	38,38953	81	1,39	IV	0,75	-86%

35	GÜMÜŞHANE	40,438588	39,508556	1219	2,77	III	1,485	-87%
36	HAKKARİ	37,583333	43,733333	1852	4,39	IV	1,84	-139%
37	HATAY	36,401849	36,34981	65	0,14	I	0,75	81%
38	IĞDIR	39,887984	44,004836	859	0,80	II	0,95	15%
39	ISPARTA	37,764771	30,556561	1054	0,58	II	1,155	50%
40	İSTANBUL	41,00527	28,97696	47	0,38	II	0,75	50%
41	İZMİR	38,41885	27,12872	6	0,13	I	0,75	83%
42	KAHRAMANMARAŞ	37,585831	36,937149	640	1,06	III	0,85	-24%
43	KARABÜK	41,2061	32,62035	312	0,82	III	0,75	-9%
44	KARAMAN	37,17593	33,228748	1039	1,14	II	1,155	1%
45	KARS	40,616667	43,1	1817	2,12	IV	1,84	-15%
46	KASTAMONU	41,38871	33,78273	784	1,64	III	1,25	-31%
47	KAYSERİ	38,73122	35,478729	1042	1,32	I	0,88	-50%
48	KIRIKKALE	39,846821	33,515251	749	0,56	II	0,85	34%
49	KIRKLARELİ	41,733333	27,216667	203	0,62	II	0,75	17%
50	KIRŞEHİR	39,14249	34,17091	1023	0,51	I	0,88	42%
51	KİLİS	36,718399	37,12122	662	0,41	II	0,75	45%
52	KOCAELİ	40,85327	29,88152	461	0,83	II	0,75	-10%
53	KONYA	37,866667	32,483333	1032	0,94	II	1,155	19%
54	KÜTAHYA	39,416667	29,983333	987	0,81	III	1,35	40%
55	MALATYA	38,35519	38,30946	945	1,14	III	1,35	16%
56	MANİSA	38,619099	27,428921	53	0,20	I	0,75	73%
57	MARDİN	37,321163	40,724477	941	0,72	II	1,05	31%
58	MERSİN	36,8	34,633333	6	0,88	I	0,75	-17%
59	MUĞLA	37,215278	28,363611	651	0,33	I	0,75	57%
60	MUŞ	38,946189	41,753893	2081	5,08	III	1,5525	-227%
61	NEVŞEHİR	38,69394	34,685651	1073	0,64	I	0,88	27%
62	NİĞDE	37,966667	34,683333	1211	1,33	II	1,155	-15%
63	ORDU	40,983879	37,876411	20	0,95	III	0,75	-27%
64	OSMANİYE	37,213026	36,176261	218	0,17	III	0,75	78%
65	RİZE	41,02005	40,523449	49	2,23	IV	0,75	-197%
66	SAKARYA	40,693997	30,435763	45	0,70	III	0,75	7%
67	SAMSUN	41,292782	36,33128	12	0,64	III	0,75	15%
68	SİİRT	37,933333	41,95	955	1,82	II	1,05	-73%
69	SİNOP	42,02314	35,153069	6	0,71	III	0,75	5%
70	SİVAS	39,747662	37,017879	1279	1,32	III	1,485	11%
71	ŞANLIURFA	37,159149	38,796909	505	0,38	I	0,75	49%
72	ŞIRNAK	37,418748	42,491834	1185	2,45	IV	1,76	-39%
73	TEKİRDAĞ	40,983333	27,516667	33	0,40	II	0,75	47%
74	TOKAT	40,316667	36,55	637	1,00	III	0,85	-18%

75	TRABZON	41,00145	39,7178	35	1,45	IV	0,75	-93%
76	TUNCELİ	39,307355	39,438778	1516	3,89	IV	1,84	-111%
77	UŞAK	38,682301	29,40819	923	0,55	II	1,05	48%
78	VAN	38,48914	43,40889	1747	1,20	IV	1,84	35%
79	YALOVA	40,65	29,266667	11	0,74	II	0,75	1%
80	YOZGAT	39,818081	34,81469	1333	1,04	III	1,485	30%
81	ZONGULDAK	41,456409	31,798731	138	1,01	III	0,75	-34%